https://doi.org/10.5194/egusphere-2026-5193
Preprint. Discussion started: 2 September 2026

Divergent predictions of northern peatland responses to climate warming and elevated CO_2: A multi-model intercomparison at the SPRUCE experiment

Xiaoying Shi[1]*, Daniel M. Ricciuto[1], Yaoping Wang[1], Joe R. Melton[2], Fortunat Joos[3,4], Yiqi Luo[5], Xiaofeng Xu[6], Dafeng Hui[7], Qianlai Zhuang[8], Chunjing Qiu[9], Hongxing He[10], Siya Shao[11], Xingjie Lu[12], Yongjiu Dai[12], Akihiko Ito[13], Qing Sun[3,4,14], Nitin Chaudhary[15], Ayesha Hussain[16], Mousong Wu[17], Jian Zhou[5], Jingwei Zhang[6], Ye Yuan[8], Rachael H. Turton[18,19], Eleanor J. Burke[18], Jiafu Mao[1], Yuefeng Hao[20], Natalie A. Griffiths[1], Verity Salmon[1], Paul J. Hanson[1], Melanie A. Mayes[1], Peter E. Thornton[1]

[1] Environmental Sciences Division, Oak Ridge National Laboratory, Oak Ridge, TN, USA,[2] Climate Research Division of Environment and Climate Change, Victoria, BC, Canada, [3]Climate and Environmental Physics, Physics Institute, University of Bern, Bern, Switzerland, [4]Oeschger Centre for Climate Change Research, University of Bern, Bern, Switzerland,[5]School of Integrative Plant Science, Cornell University, Ithaca, NY, USA, [6]Biology Department, San Diego State University, San Diego, CA, USA, [7]Department of Biological Sciences, Tennessee State University, Nashville, TN, USA, [8]Department of Earth, Atmospheric, and Planetary Sciences, Department of Agronomy, Purdue University, West Lafayette, IN, USA,[9]Research Center for Global Change and Ecological Forecasting, School of Ecological and Environmental Sciences, East China Normal University, Shanghai, China,[10]Department of Geography, McGill University, Montréal, Québec, Canada,[11] Department of Microbiology, University of Tennessee, Knoxville, TN, USA, [12]School of Atmospheric Sciences, Sun Yat-Sen University, Guangzhou, China, [13]The University of Tokyo, Tokyo, Japan,[14]Wyss Academy for Nature, University of Bern, Bern, Switzerland ,[15]Department of Earth and Environmental Sciences, Lund University, Lund, Sweden, and Stockholm Resilience Centre, Stockholm University, Stockholm, Sweden, [16]University of Exeter, Exeter, UK, [17]International Institute for Earth System Science, Nanjing University, Nanjing, China, [18]Met Office Hadley Centre, Exeter, UK, [19]UK Centre for Ecology and Hydrology, Wallingford, UK, [20]Department of Industrial and Systems Engineering, University of Tennessee, Knoxville, TN, USA

*Corresponding author: Xiaoying Shi (shix@ornl.gov)

https://doi.org/10.5194/egusphere-2026-5193
Preprint. Discussion started: 2 September 2026

Abstract

Peatlands cover only ~3% of Earth's land surface yet store ~30% of global soil carbon (C), making them critical components of the terrestrial C cycle and influential regulators of C-climate feedbacks. However, their responses to climate warming and elevated CO_2 remain highly uncertain, in part because Earth system models represent peatland processes with varying levels of complexity and realism, and because peat C pools turn over on centennial to millennial timescales that challenge model evaluation. Here, we present results from the SPRUCE (Spruce and Peatland Responses Under Changing Environments) Model Intercomparison Project (SPRUCE-MIP), which evaluates 15 terrestrial ecosystem models against observations from a long-term whole-ecosystem warming and CO_2-enrichment experiment at an ombrotrophic bog in northern Minnesota, USA. Models were driven by observed meteorology from in situ warming treatments spanning +0 to +9 °C, at either ambient or elevated CO_2 (+500 ppm). Simulated net ecosystem exchange (NEE), net primary productivity (NPP), heterotrophic respiration (HR), and methane (CH_4) fluxes were benchmarked against multi-year observations. Model predictions exhibit a large spread in both baseline C balance, ranging from strong sinks to strong sources under +0 °C warming, and temperature sensitivity, indicating substantial uncertainty in predicting peatland C responses to environmental forcing. Across the ensemble, models fall into four distinct functional response types: (i) models that simulate peatlands as net C sources across all warming and CO_2 conditions; (ii) models that transition from C sinks to sources under warming irrespective of CO_2 level; (iii) models that transition only under ambient CO_2 but remain C sinks under elevated CO_2, reflecting strong CO_2 fertilization effects; and (iv) models that maintain persistent sinks or near-neutral C balance even under extreme warming. While most models predict enhanced NPP under elevated CO_2 across all warming treatments, SPRUCE observations show little or no NPP enhancement under elevated CO_2 at the +0 and +2.25 °C warming levels, with a positive CO_2 fertilization effect emerging only under stronger warming. This discrepancy highlights persistent model biases in representing interactions between warming and CO_2 responses. Process-based analysis further indicates that divergence in modeled responses is associated with differences in vegetation structure (light competition and moss representation), nutrient cycling (nitrogen and phosphorus), and dynamic peat representation. These structural differences systematically influence ecosystem productivity, heterotrophic respiration, and net C balance across the model ensemble. An illustrative parameter sensitivity analysis using the SPRUCE-specific Energy

https://doi.org/10.5194/egusphere-2026-5193
Preprint. Discussion started: 2 September 2026

Exascale Earth System Model (E3SM) Land Model (ELM-SPRUCE) further shows that parameter choices can also modulate the magnitude of simulated responses. Together, these results demonstrate that peatland responses to warming and elevated CO_2 are highly sensitive to model structure, parameterization, and process coupling, highlighting the need for improved representation of key peatland processes to reduce uncertainty in Earth system projections. The SPRUCE experimental framework provides a unique benchmark for evaluation and improving process representation and constraining near-term peatland response to environmental change, thereby strengthening confidence in longer-term C-climate projections.

Keywords: peatland carbon cycling; climate warming; elevated CO_2; methane emissions; ecosystem modeling

1. Introduction

Recent synthesis efforts and observational datasets continue to highlight the large-scale carbon (C) storage role of northern peatlands (Crichton et al., 2025; Loisel et al., 2021; Treat et al., 2014). Due to slow organic matter decomposition under anoxic and water-saturated conditions, peatlands have accumulated large stores of soil C over millennia (Yu, 2012). Thus, despite occupying ~ 3% of the Earth's terrestrial surface, these unique and climate sensitive ecosystems account for about one third of the terrestrial soil C pool (Dargie et al., 2017; Leifeld and Menichetti, 2018; Ribeiro

https://doi.org/10.5194/egusphere-2026-5193
Preprint. Discussion started: 2 September 2026

et al., 2021; Skye et al., 2026; Xu et al., 2018). This long-term C storage capacity underscores the outsized role of peatlands in regulating earth system and highlights the need to improve mechanistic understanding and predictive capacity by integrating observations with process-based modeling (Duque et al., 2021; Treat et al., 2014).

While intact peatlands generally function as net C sinks, warming, permafrost thaw, water table fluctuations, and anthropogenic disturbance can shift them to net sources of greenhouse gases (Frolking et al., 2011; (IPCC), 2023; Loisel et al., 2021; Zhao and Zhuang, 2023). Empirical projections based on relationships between peat carbon accumulation over the last millennium and climate suggest that, under two Representative Concentration Pathway (RCP) scenarios (RCP2.6 and RCP8.5), the global peatland C sink may initially strengthen with warming but begin to weaken around the end of the 21st century, shifting the peatland response toward a positive climate feedback (Gallego-Sala et al., 2018). Consistent with these projections, warming experiments in boreal peatlands have reported CO_2 and CH_4 emissions several times higher than historical C accumulation rates (Hanson et al., 2020). Warming-induce decrease in peatland water tables further reveals complex, and sometimes opposing responses, with increases in CO_2 emissions partially offset by decreases in CH_4 emissions, with variable impacts on gross primary productivity (GPP) (Huang et al., 2021; Kwon et al., 2022; McDonald et al., 2023). Additional drivers including changes in litter inputs and soil decomposition rates, seasonally differing warming rates, permafrost degradation, and fire further complicate peatland C dynamics (Helbig et al., 2022; O'Donnell et al., 2012; Ofiti et al., 2023; Qiu et al., 2020; Turetsky et al., 2011).

Accurate modeling of observed peatland C responses to environmental change is challenging due to strong nonlinearities and threshold behavior arising from interactions among the underlying processes driving microbial decomposition rates, vegetation turnover, and water table dynamics (Hedwall et al., 2017; Helbig et al., 2020). An additional challenge is representing the legacy effects of past climatic and environmental changes, given that peatland C accumulation and turnover operate on timescales ranging from years to millennia (Müller and Joos, 2021). Modeling CH_4 emissions remains particularly uncertain due to challenges in representing anaerobic microbial pathways, substrate availability, and hydrological controls (Estop-Aragonés et al., 2018; Melton et al., 2013). Recent modelling studies further emphasize the importance of trait-based vegetation dynamics and microbial-explicit process representation to capture peatland warming

https://doi.org/10.5194/egusphere-2026-5193
Preprint. Discussion started: 2 September 2026

responses (Shi et al., 2021; Wang et al., 2026; Zhao et al., 2022). To address these challenges, a range of process-based peatland models have been developed to simulate the effects of temperature, precipitation, vegetation shifts, and permafrost dynamics. For instance, LPJ-GUESS incorporates peatland processes to simulate long-term C accumulation under future scenarios (Chaudhary et al., 2017). ORCHIDEE has been applied to assess century-scale peatland C fluxes (Qiu et al., 2019), while the Holocene Peatland Model (HPM) reconstructs long-term development and climate sensitivity over millennial timescales (Frolking et al., 2014; Treat et al., 2021). However, evaluating these models remains challenging because the relatively short duration of observational and experimental records contrasts with the long intrinsic timescales of peat carbon accumulation, complicating model spin-up, initialization, and assessment of longer-term C-climate feedbacks. This timescale mismatch further motivates coordinated model-experiment intercomparisons such as the Spruce and Peatland Responses Under Changing Environments (SPRUCE) Model Intercomparison Project (SPRUCE-MIP) to evaluate how models translate near-term ecosystem responses into longer-term carbon-climate feedbacks.

Despite decades of progress in peatland ecosystem modeling (Chaudhary et al., 2020, 2026; Frolking et al., 2010, 2014; Müller and Joos, 2021; Treat et al., 2021; Wania et al., 2009; Zhao and Zhuang, 2023, 2024) substantial uncertainty remains in projecting peatland C dynamics under future environmental change. Earlier model intercomparison projects, including WETCHIMP and WETCHIMP-WSL, revealed large divergence in simulated peatland CH_4 emissions, primarily because of differences in hydrological, vegetation, and microbial process representations (Bohn et al., 2015; Melton et al., 2013). More recent studies similarly project widely varying 21st-century peatland C balances. Some models predict transitions from long-term C sinks to net C sources under moderate to high greenhouse-gas emission scenarios (e.g., RCP4.5 and RCP8.5) (Chaudhary et al., 2017; Müller and Joos, 2021; Zhao and Zhuang, 2023, 2024), whereas others project reduced sink strength or continued net C uptake under comparable or lower forcing scenarios (Chaudhary et al., 2020; Qiu et al., 2020). These contrasting projections reflect differences in the representation of nutrient cycling, vegetation dynamics, peatland hydrology, and CH_4 production, oxidation, and transport, as well as in how these processes are coupled within models. Consequently, it remains unclear which ecosystem processes exert the strongest controls on peatland C responses to combined warming and elevated CO_2.

https://doi.org/10.5194/egusphere-2026-5193
Preprint. Discussion started: 2 September 2026

To systematically evaluate and benchmark model performance under observed warming and CO_2 enrichment, the SPRUCE-MIP was launched. SPRUCE-MIP assesses how diverse terrestrial ecosystem models simulate C cycle responses using a common experimental protocol at the SPRUCE site. The SPRUCE experiment combines whole-ecosystem warming and elevated CO_2 (eCO_2) treatments at an ombrotrophic bog in northern Minnesota, USA. Site-based whole-ecosystem manipulative experiments like SPRUCE provide uniquely powerful testbeds to evaluate model predictions under controlled, yet ecologically realistic conditions (Hanson et al., 2017, 2020; Norby et al., 2016). The goals of SPRUCE-MIP are to identify sources of uncertainty, benchmark model performance against multi-year observations, and guide future improvements in peatland process representation.

This paper presents the SPRUCE-MIP framework, including site information, the modelling protocol, model forcing and observational datasets, the metrics used to compare model simulations with observations, and the participating models (Section 2). Section 3 presents model performance and examines how differences in process representation contribute to divergent model responses. Section 4 discusses the implications of these findings for model uncertainty, peatland C-climate feedbacks, and future model development, and Section 5 summarizes the main conclusions.

2. Methodology

2.1 Site information

SPRUCE examines peatland ecosystem responses to multiple levels of whole-ecosystem warming under both ambient and elevated CO_2 conditions (aCO_2 and eCO_2, respectively) (Hanson et al., 2017). This experiment is conducted within the S1 bog, an 8.1-hectare peatland. The S1 Bog is a raised, ombrotrophic bog in northern Minnesota, USA, within the Marcell Experimental Forest that is managed by the United States Department of Agriculture Forest Service (47°30.476′ N, 93°27.162′ W). The mean annual temperature at the S1 bog was 3.4 °C and the average annual precipitation was 780 mm for the period 1961-2009, reflecting its boreal climate characteristics (Sebestyen et al., 2011). The overstory vegetation is primarily composed of black spruce (*Picea mariana*) and tamarack (*Larix laricina*), underlain by a dense Sphagnum moss layer (dominated by *S. divinum*, *S. angustifolium*, and *S. fallax*). The understory features a variety of shrubs

https://doi.org/10.5194/egusphere-2026-5193
Preprint. Discussion started: 2 September 2026

including Labrador tea (*Rhododendron groenlandicum*) and leatherleaf (*Chamaedaphne calyculata*), along with a few herbaceous and graminoid species (Hanson et al., 2020).

The SPRUCE experiment uses open-top enclosures (12.8 m in diameter and 7m in height) in which propane-warmed air is circulated through a system of air handling units as well as soil heaters to apply whole ecosystem-warming to both the atmosphere and deep peat soils (Hanson et al., 2017). These enclosures enabled simultaneous warming across five temperature increments: +0°C, +2.25°C, +4.5°C, +6.75°C, and +9°C. These warming levels reflect target temperature offsets that are actively controlled in the field using continuous feedback-based heating systems. As a result, the specified temperature differences should be interpreted as time-averaged offsets that emerge over sub-daily to seasonal timescales, rather than exact instantaneous temperature differences (Hanson et al., 2017) . In addition to the ten treatment enclosures, an unchambered ambient plot (Plot 7) was used as the control, representing ambient meteorological and CO_2 conditions without enclosure effects.

Soil warming was implemented using resistance heaters extending to a depth of 3 m following Hanson et al. (2017), with deep peat warming applied while minimizing direct heating of the shallow peat layers. Each warming treatment was evaluated under both aCO_2 and eCO_2 conditions, with eCO_2 targeting an enrichment of approximately 500 ppm above ambient concentrations (resulting in atmospheric CO_2 concentrations of approximately 800–900 ppm). Whole-ecosystem warming began in August 2015, followed by eCO_2 treatment in June 2016. Because each warming × CO_2 treatment was applied to a single enclosure, spatial variability among plots cannot be statistically separated from treatment effects. Nevertheless, multi-year averaging reduces the influence of short-term variability, and the imposed temperature offsets are substantially larger than background interannual climate variability (Hanson et al., 2017).

2.2. Modelling protocol

The models participating in SPRUCE-MIP followed a common modelling protocol described here and summarized in Table 1. During the initial spin-up phase, each model was driven to equilibrium under pre-industrial conditions by repeatedly cycling the 2015-2021 atmospheric forcing data from the control plot, while holding CO_2 concentration, nitrogen deposition, land use and land cover

https://doi.org/10.5194/egusphere-2026-5193
Preprint. Discussion started: 2 September 2026

constant at their 1850 values. This was followed by a transient simulation covering 1850 to 2014. Finally, measured plot-level meteorological forcing from the control plot and the ten treatment enclosures was used to drive the 11 experimental simulations evaluated during the 2015-2021 observation period (Table 1). These simulations were compared with the corresponding observational datasets collected during the same period.

The evaluation consisted of 11 simulations: a control simulation without an enclosure and ten enclosure simulations representing five warming treatments under both aCO_2 and eCO_2 conditions (Table 1). Specifically, the temperature treatments, as discussed in Section 2.1, were set at increments of +0 °C, +2.25 °C, +4.5 °C, +6.75 °C, and +9 °C, applied under aCO_2 and eCO_2 (+500 ppm) conditions.

In addition, the simulations accounted for a major strip cutting event in 1974, represented as a 99% reduction in aboveground tree biomass, exclusive of shrubs or moss (Hanson et al., 2025), reflecting the extensive strip cuts conducted within the experimental forest during that period.

Table 1. Overview of the SPRUCE-MIP experimental simulations used for model evaluation during 2015-2021.

Simulation	Period	Warming	Atmospheric CO_2	Description
Control (CTL)	2015-2021	ambient	ambient	Control plot in its natural state without any enclosure.
T0.00 aCO_2	2015-2021	+0ºC	ambient	Baseline warming treatment under aCO_2 inside an enclosure.
T2.25 aCO_2	2015-2021	+2.25ºC	ambient	Mild warming treatment under aCO_2 inside an enclosure.
T4.50 aCO_2	2015-2021	+4.50ºC	ambient	Moderate warming treatment under aCO_2 inside an enclosure.
T6.75 aCO_2	2015-2021	+6.75ºC	ambient	High warming treatment under aCO_2 inside an enclosure.
T9.00 aCO_2	2015-2021	+9.00ºC	ambient	Extreme warming treatment under aCO_2 inside an enclosure.
T0.00 eCO_2	2015-2021	+0ºC	ambient+500ppm	Baseline warming treatment under eCO_2 inside an enclosure.
T2.25 eCO_2	2015-2021	+2.25ºC	ambient+500ppm	Mild warming treatment under eCO_2 inside an enclosure.
T4.50 eCO_2	2015-2021	+4.50ºC	ambient+500ppm	Moderate warming treatment under eCO_2 inside an enclosure.
T6.75 eCO_2	2015-2021	+6.75ºC	ambient+500ppm	High warming treatment under eCO_2 inside an enclosure.
T9.00 eCO_2	2015-2021	+9.00ºC	ambient+500ppm	Extreme warming treatment under eCO_2 inside an enclosure.

https://doi.org/10.5194/egusphere-2026-5193
Preprint. Discussion started: 2 September 2026

2.3. Datasets

2.3.1 Model forcing datasets

Models were driven by the observed plot-level meteorological forcing, including air temperature, precipitation, wind speed, atmospheric pressure, relative humidity, and incoming longwave and shortwave radiation. Water table depth was also provided for the models that required this variable as a driver. Additional details about the collection of these plot-scale forcing datasets can be found in Hanson et al. (2016, 2017).

Fig.1 shows the multi-year mean annual air temperature for the ten treatment enclosures together with the control plot in its natural state without enclosure during 2015-2021. The temperature difference between plot6 (enclosed control) and plot7 (unenclosed control) reflects the influence of the enclosure itself, with the unenclosed plot exhibiting lower mean annual temperature. This temperature difference likely arises from passive chamber effects, including changes in incoming shortwave and longwave radiation and altered air circulation associated with the blower system (Hanson et al., 2017).

https://doi.org/10.5194/egusphere-2026-5193
Preprint. Discussion started: 2 September 2026

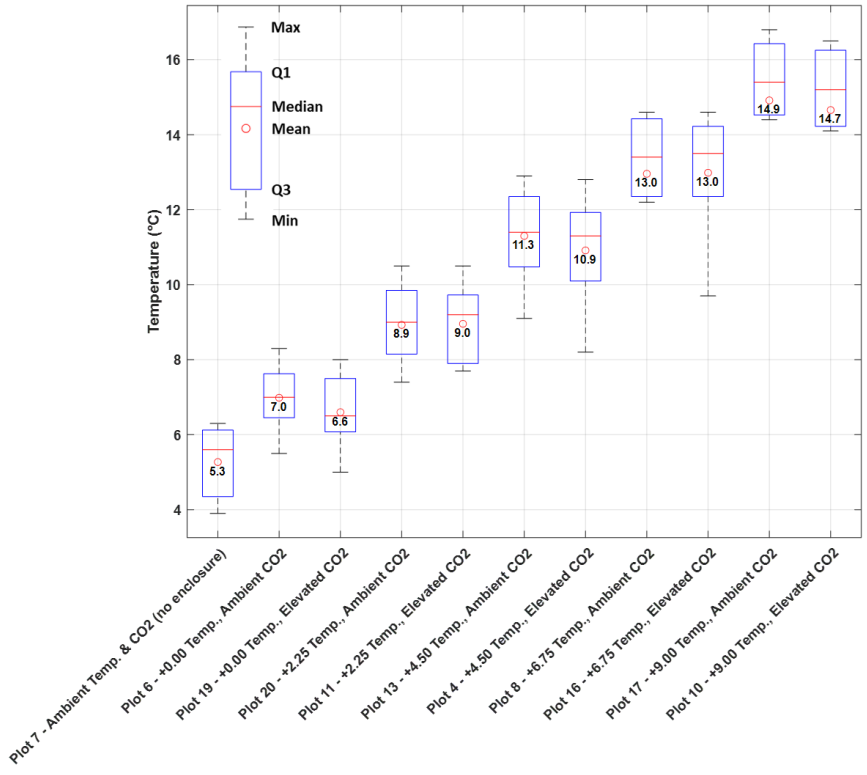

Fig. 1. Multi-year mean annual air temperature across the eleven SPRUCE plots during 2015-2021, including the unenclosed control plot and ten enclosures representing five warming levels under ambient and elevated CO_2 conditions.

2.3.2 Observational datasets

The observational datasets used in this study span the 2015-2021 experimental period and include annual net ecosystem exchange (NEE; g C m^{-2} yr^{-1}), heterotrophic respiration (HR; g C m^{-2} yr^{-1}), methane (CH_4; g C m^{-2} yr^{-1}) emissions, and net primary productivity (NPP; g C m^{-2} yr^{-1}) for each experimental plot. Negative NEE values indicate net carbon uptake by the ecosystem, whereas positive values indicate net carbon release to the atmosphere.

The annual NPP for each plot was derived from measured biomass following the methods described by Griffiths et al. (2017) and Hanson et al. (2020). Total annual NPP was calculated as the sum of aboveground NPP from trees and shrubs, including foliar production associated with

https://doi.org/10.5194/egusphere-2026-5193
Preprint. Discussion started: 2 September 2026

annual litterfall, NPP of the *Sphagnum* community, and annual belowground contributions from fine roots. Annual shrub stem and coarse-root increments were not measured and was assumed to contribute only a small fraction of total NPP (Hanson et al., 2020).

Carbon dioxide (CO_2) and methane (CH_4) fluxes were measured using in situ chamber methods following Hanson et al. (2016, 2017). Measurements were made approximately monthly during the growing season (day of year 122-244; (Richardson et al., 2018)), with additional sampling during selected dormant-season periods. One pairs of permanent collars were installed within each plot and embedded 10–20 cm into the peat surface. CO_2 exchange was measured using both transparent chambers (NEE) and darkened chambers (ecosystem respiration). NEE was partitioned into heterotrophic (HR) and autotrophic respiration (AR) using off-plot vegetation-clipping experiments. HR observations were incorporated into the ecosystem carbon balance because plant carbon dynamics were represented independently through the observed aboveground and belowground NPP components described above. Chamber measurements were also used to estimate CH_4 emissions. Additional details on measurement protocols and data processing are provided by Hanson et al. (2020).

2.4 Metrics for comparison between observations and model simulations

Model simulations were first compared with observations from the +0.00 treatment to evaluate baseline model performance at the SPRUCE site. Temperature sensitivities of C fluxes were quantified using least-squares linear regression between annual mean air temperature and annual mean ecosystem C fluxes, including NEE, NPP, HR, and CH_4 fluxes. For each plot and model simulation, annual mean air temperatures and fluxes were computed for each year during the 2015-2021 experimental period. Regressions were performed across all years and warming treatments separately for aCO_2 and eCO_2 conditions. The resulting regression slopes represent emergent, time-averaged sensitivities to warming across the imposed temperature gradients, rather than instantaneous or process-level responses. Uncertainty in the estimated sensitivities was quantified as ±1 standard deviation of the regression slope following standard linear regression theory (DeGroot and Schervish, 2018). Temperature sensitivities were calculated consistently for observations and all participating models to facilitate direct comparison. An example of the regression-based estimation of temperature sensitivity for observed NEE is shown in Fig. S1.

https://doi.org/10.5194/egusphere-2026-5193
Preprint. Discussion started: 2 September 2026

Because each warming × CO_2 treatment was implemented in a single enclosure, annual values reflect temporal variability rather than independent spatial replication across treatments. Therefore, the estimated slopes were used to characterize emergent warming sensitivities and to test whether individual slopes differ from zero, but formal tests comparing observed slopes between aCO_2 and eCO_2 treatments, or comparing model slopes directly against observational slopes, were not applied. Such tests would require stronger assumptions about independence among treatment enclosures than are supported by the experimental design.

2.5 Participating models

SPRUCE-MIP includes 15 terrestrial ecosystem models with diverse structures and process complexities (Table 2), including: CLASSIC (Melton et al., 2020), CLM-Microbe (Xu et al., 2015), CoLM (Dai et al., 2019), CoupModel (He et al., 2021), DNDC (Li et al., 1992), ELM-Microbe (Ricciuto et al., 2021), ELM-SPRUCE (Shi et al., 2021), JULES (Mathison et al., 2023), LPX-Bern (Spahni et al., 2013), LPJ-GUESS (Chaudhary et al., 2017), MWM (Shao et al., 2022, 2023; St-Hilaire et al., 2010), ORCHIDEE (Qiu et al., 2017, 2019), TECO-SPRUCE (Huang et al., 2017; Weng and Luo, 2008), PTEM (Zhao and Zhuang, 2024), and VISIT (Ito and Inatomi, 2012).

All participating models simulate core ecosystem processes including energy, water and carbon cycles, although their structure, parameterizations, and complexity vary. Figure 2 summarizes the representation of nine peatland-relevant processes across the participating models, illustrating similarities and differences in structural complexity These include acclimation (ACC; applied to photosynthesis and/or decomposition), predicted water table dynamics (PWT), methane cycling (CH_4), moss representation (Moss), nutrient cycling (nitrogen and phosphorus), light competition by different plant types (Light), dynamic peat depth (Peat), and microtopography (MT).

Figure 2 reveals substantial diversity in process representation across the participating models. ELM-Microbe, CLM-Microbe, and ELM-SPRUCE incorporate the largest number of evaluated peatland-relevant processes, whereas models such as CoLM and TECO-SPRUCE represent a more limited subset. Intermediate-complexity models, including LPX-Bern and PTEM, incorporate many key peatland processes while omitting others, such as phosphorus cycling, acclimation, or

https://doi.org/10.5194/egusphere-2026-5193
Preprint. Discussion started: 2 September 2026

317 microtopography. Overall, the participating models span a broad range of structural
318 configurations, providing a useful basis for evaluating how differences in process representation
319 contribute to divergent model behavior.

320 Below are brief descriptions of each model, emphasizing structural features most relevant to the
321 SPRUCE-MIP intercomparison.

322 • **CLASSIC** (v1.5) incorporates peatland-specific vegetation, Sphagnum moss, dynamic
323 peat depth, and water table dynamics. Nitrogen and CH_4 modules were disabled for this
324 study.
325 • **CLM-Microbe** builds on the CLM4.5 framework (Oleson et al., 2013) and incorporates
326 microbial functional groups and methane cycling. It represents an early version of ELM-
327 Microbe.
328 • **CoLM** includes updated biogeochemical routines and plant water and nitrogen
329 competition but does not explicitly represent peatland and methane processes.
330 • **CoupModel** simulates coupled soil–plant–atmosphere heat, water, and carbon exchanges
331 and has been applied to both pristine and disturbed peatlands.
332 • **DNDC** simulates coupled carbon and nitrogen cycling and greenhouse-gas emissions. For
333 this study, the Forest-DNDC configuration was initialized without separate spin-up or
334 historical transient simulations.
335 • **ELM-Microbe** extends the ELM framework with explicit microbial decomposition and
336 methane dynamics.
337 • **ELM-SPRUCE** integrates ELM vegetation and hydrology with CLM4Me-based methane
338 dynamics (Riley et al., 2011) and peatland-specific representations of hydrology,
339 microtopography, and Sphagnum moss.
340 • **JULES** simulates terrestrial carbon and water exchange but omits moss and peatland-
341 specific structural components.
342 • **LPX-Bern** is a dynamic global vegetation model with coupled water, carbon, and nitrogen
343 cycling and an explicit global peatland representation.
344 • **LPJ-GUESS** is an individual- and patch- dynamic based vegetation model with explicit
345 representations of peatland and permafrost processes.

https://doi.org/10.5194/egusphere-2026-5193
Preprint. Discussion started: 2 September 2026

- **MWM** includes peat accumulation, microbial decomposition, and nutrient cycling, emphasized for long-term peat development.
- **ORCHIDEE-Peat** explicitly represents peatland carbon, hydrology and vegetation dynamics; methane processes were disabled for this study.
- **TECO-SPRUCE** adapts the TECO model for SPRUCE, incorporating carbon-nitrogen coupling, methane processes, and water table dynamics.
- **PTEM** simulates peatland carbon and nitrogen dynamics, including plant functional types, water table dynamics, methane cycling, peat accumulation, and aerobic and anaerobic decomposition.
- **VISIT** simulates trace-gas fluxes, including methane emissions, using environmentally and empirically constrained drivers.

Each model reflects a distinct set of assumptions regarding peatland biogeochemistry and ecosystem functioning. These structural differences provide the foundation for the process-based analyses presented in Sections 3.3 and 4.3. Modifications made specifically for SPRUCE-MIP beyond previously published model versions are described in the Supplementary Material. Unless otherwise noted, all models followed the standardized SPRUCE-MIP protocol described in Section 2.2 and Table 1.

Table 2. Participating models in SPRUCE-MIP.

Model Name	Full Name	Affiliation (Team Contact)	References
CLASSIC	Canadian Land Surface Scheme Including Biogeochemical Cycles	Environment and Climate Change Canada (Joe Melton)	(Melton et al., 2020)
CLM-Microbe	Community Land Model with Microbial Processes	San Diego State University (Xiaofeng Xu)	(Xu et al., 2015)
CoLM	Common Land Model	Sun Yat-Sen University (Xingjie Lu)	(Dai et al., 2019)
CoupModel	Coupled Heat and Mass Transfer Model	McGill University (Hongxing He)	(Jansson and Moon, 2001)
DNDC	DeNitrification-DeComposition Model	Tennessee State University (Dafeng Hui)	(Li et al., 1992)
ELM-Microbe	Energy Exascale Earth System Model (E3SM) Land Model (ELM) with Microbial Processes	San Diego State University (Xiaofeng Xu)	(Ricciuto et al., 2021)
ELM-SPRUCE	Energy Exascale Earth System Model (E3SM) Land	Oak Ridge National Laboratory (Xiaoying Shi)	(Shi et al., 2021)

https://doi.org/10.5194/egusphere-2026-5193
Preprint. Discussion started: 2 September 2026

	Model (ELM) with SPRUCE-specific processes		
JULES	Joint UK Land Environment Simulator	University of Exeter (Ayesha Hussain)	(Mathison et al., 2023)
LPX-Bern	Land surface Processes and eXchanges model	University of Bern (Qing Sun/Fortunat Joos)	(Spahni et al., 2013)
LPJ-GUESS	Lund-Postsdam-Jena GeneralEcosystem Simulator	Lund University (Nitin Chaudhary)	(Chaudhary et al., 2017)
MWM	McGill Wetland Model	McGill University (Siya Shao)	(Shao et al., 2022, 2023; St-Hilaire et al., 2010)
ORCHIDEE-Peat	ORganizing Carbon and Hydrology In Dynamic Ecosystems model	East China Normal University (Chunjing Qiu)	(Qiu et al., 2017, 2019)
TECO-SPRUCE	Terrestrial ECOsystem Model	Cornell University (Jian Zhou, Yiqi Luo)	(Huang et al., 2017; Weng and Luo, 2008)
PTEM	Peatland Terrestrial Ecosystem Model	Purdue University (Qianlai Zhuang)	(Zhao and Zhuang, 2024)
VISIT	Vegetation Integrative SImulator for Trace gases	University of Tokyo (Akihiko Ito)	(Ito and Inatomi, 2012)

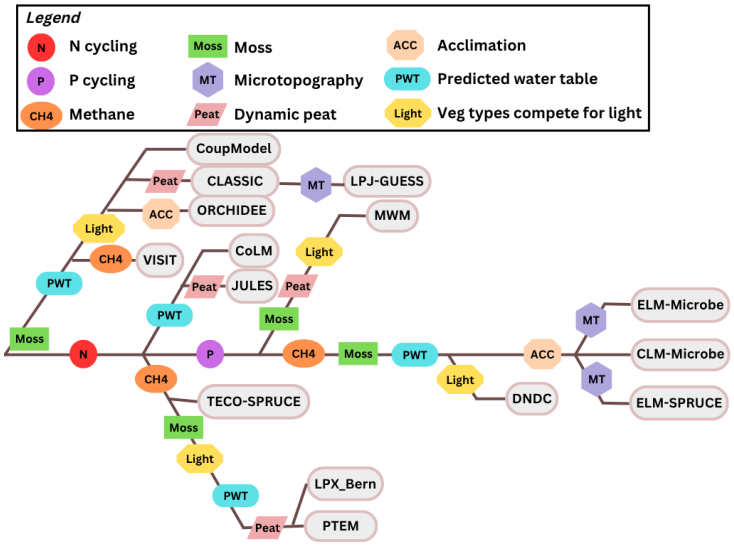

364

365 **Fig. 2**. Tree diagram illustrating differences in the representation of nine peatland-relevant
366 ecosystem processes across the 15 participating models. Branch points indicate the inclusion of
367 specific processes (colored symbols; see legend), highlighting similarities and differences in
368 structural complexity that provide the basis for the process-based analyses presented in Sections
369 3.3 and 4.3.

370 **3. Results**

https://doi.org/10.5194/egusphere-2026-5193
Preprint. Discussion started: 2 September 2026

3.1 Simulated net ecosystem carbon exchange and its components

Under baseline (+0 °C) warming, observations indicate that the S1 bog peatland functions as a weak C source under both CO_2 treatments, with multi-year mean NEE of 44±68 and 58±56 gC m^{-2} yr^{-1} under aCO_2 and eCO_2, respectively (Fig.3a). The large interannual variability relative to mean NEE indicates that the peatland functions as a weak carbon sink in some years. Only four of fifteen models (CoupModel, ELM-Microbe, LPX-Bern and PTEM) reproduce a positive (source) mean NEE, though their magnitudes differ under both CO_2 conditions. For example, LPX-Bern simulates a small positive NEE under both aCO_2 (14±66 gC m^{-2} yr^{-1}) and eCO_2 (11±43 gC m^{-2} yr^{-1}), while ELM-Microbe produces substantial a larger positive NEE (199±132 gC m^{-2} yr^{-1} for aCO_2 and 83±135 gC m^{-2} yr^{-1} for eCO_2). CLASSIC transitions from a near-neutral source (+5±17 gC m^{-2} yr^{-1}) under aCO_2 to a modest sink (-38±25 gC m^{-2} yr^{-1}) under eCO_2 with simulated values remaining broadly consistent with the observational uncertainty range. Similarly, CLM-Microbe switches from a near-neutral sink (-11±79 gC m^{-2} yr^{-1}) under aCO_2 to a modest source (50±86 gC m^{-2} yr^{-1}) under eCO_2. The remaining nine models all simulate net C uptake, with DNDC showing particularly high sequestration. Overall, the multi-model mean indicates an approximately 142% increase in net C uptake under eCO_2 relative to aCO_2, whereas observations suggest slightly greater C loss under eCO_2. Exceptions include CLM-Microbe, which also simulates enhanced carbon loss under eCO_2, and CoupModel and LPX-Bern, which exhibit minimal sensitivity to CO_2 enrichment. However, the apparent divergence between simulated and observed CO_2 responses should be interpreted with caution given the substantial observational uncertainty. Pretreatment NEE, estimated using circular collars in a manner consistent with the post-treatment values used in this study (Sect. 2.3.2), exhibits a standard deviation equal to about 100% of the mean source strength (Hanson et al., 2020), which is larger than the observed difference between the aCO_2 and eCO_2 treatments (Fig. 3a).

Fig.3b illustrates the diversity of simulated NPP across models relative to observations under both CO_2 conditions. The multi-year mean observed NPP is approximately 355±47 gC m^{-2} yr^{-1} (aCO_2) and 345±60 gC m^{-2} yr^{-1} (eCO_2). The slightly lower observed NPP under eCO_2, estimated through biomass instead of circular collars, is consistent with the higher NEE source strength above, despite observational uncertainties. The predicted NPP from CLM-Microbe aligns closely with the

https://doi.org/10.5194/egusphere-2026-5193
Preprint. Discussion started: 2 September 2026

observations. The multi-model mean NPP exceeds observed values slightly, but this modest overestimation is expected, given that some models may include shrub stem and coarse-root increments in their NPP estimates (Sect. 2.3.2). Seven models (CoupModel, CLASSIC, ELM-SPRUCE, LPJ-GUESS, MWM, ORCHIDEE and PTEM) underestimate NPP, and the other seven models (CoLM, DNDC, ELM-Microbe, LPX-Bern, JULES, TECO-SPRUCE and VISIT) overestimate it, especially under eCO_2. Most models predict higher NPP under eCO_2 than aCO_2, with exceptions being CLM-Microbe and LPX-Bern. Particularly notable NPP increases under eCO_2 conditions are observed in the ORCHIDEE (139%), VISIT (105%), ELM-Microbe (64%), LPJ-GUESS (50%) and DNDC (47%) models. An increase in observed NPP under eCO_2 is not evident at +0 °C and +2.25°C but emerges under stronger warming (Figs. S2-S5).

Observed HR is 348±26 gC m^{-2} yr^{-1} (aCO_2), and 357±20 gC m^{-2} yr^{-1} (eCO_2), indicating little sensitivity to eCO_2 (Fig. 3c). The multi-model mean, as well as simulations from CoupModel, PTEM and VISIT, fall within the ± standard deviation range of the HR observations. In contrast, CLM-Microbe, CLASSIC, DNDC, ELM-SPRUCE, LPJ-GUESS, MWM, and ORCHIDEE underestimate HR. In particular, CLASSIC, DNDC and MWM predict relatively low HR (generally < 90 gC m^{-2} yr^{-1}). Conversely, CoLM, ELM-Microbe, JULES, LPX-Bern, and TECO-SPRUCE substantially overestimate HR, with simulated values generally ranging from ~490 to 800 gC m^{-2} yr^{-1}. Several models, including ELM-Microbe, LPJ-GUESS, MWM, ORCHIDEE and TECO-SPRUCE exhibit strong eCO_2-driven increases in HR, while other models show limited short-term HR responses to eCO_2 during the experimental period (Fig.3c).

The observed CH_4 fluxes are 21±11 gC m^{-2} yr^{-1} (aCO_2) and 24±13 gC m^{-2} yr^{-1} (eCO_2), indicating an approximately 15% increase under eCO_2 (Fig. 3d). Among the nine models that simulate CH_4 fluxes, VISIT predicts values closest to observations, with differences within ±3 gC m^{-2} yr^{-1}. LPX-Bern and ELM-SPRUCE substantially underestimate CH_4 emissions, whereas CLM-Microbe, LPJ-GUESS, DNDC, ELM-Microbe, PTEM and TECO-SPRUCE overestimate CH_4 fluxes under both aCO_2 and eCO_2 conditions generally by more than 6 gC m^{-2} yr^{-1}. Relative to their aCO_2 simulations, CLM-Microbe shows the largest increase in CH_4 flux under eCO_2 (~81% higher), followed by TECO-SPRUCE (~29% higher). In contrast, PTEM predicts a ~14% decrease in CH_4 flux under eCO_2 relative to aCO_2 (Fig. 3d).

https://doi.org/10.5194/egusphere-2026-5193
Preprint. Discussion started: 2 September 2026

Supplemental Figs. S2-S5 show how increasing warming modifies these baseline responses described above across the full experimental temperature gradient. Because high-latitude regions experience amplified warming relative to the global mean, the higher-warming treatments (+4.5 °C and above) are broadly representative of plausible future climatic conditions at the SPRUCE site under projected global warming of ~1-2 °C during the 21st century (Xie et al., 2022). Observations of NEE at higher warming levels (particularly +9 °C, 410±165 gC m^{-2} yr^{-1} for aCO_2 and 308±139 gC m^{-2} yr^{-1} for eCO_2) suggest that the peatland transitions toward a stronger C source. Consistent with this pattern, the four models that already predict positive NEE at +0 °C (CoupModel, ELM-Microbe, LPX-Bern and PTEM) generally show larger C losses with warming than the models predicting neutral or negative NEE under baseline conditions. CLASSIC shifts from near-neutral or weak C sink (under eCO_2)/source (under aCO_2) at lower warming (+0 and +2.25°C) to a weak C source across the +4.50 °C to +9°C warming levels under both CO_2 conditions, with multi-year mean source or sink magnitudes remaining within ± 60 gC m^{-2} yr^{-1}, substantially smaller than the observed source strengths under strong warming. LPJ-GUESS transitions from a very weak sink to a very weak source under both CO_2 conditions beginning at +4.50°C, with sources/sinks magnitudes always within ± 30 gC m^{-2} yr^{-1}. Several models transition from C sinks to sources only at higher warming levels. ELM-SPRUCE shifts from a C sink to a source under both CO_2 scenarios starting from +6.75°C, whereas CoLM does so only at +9°C. JULES, ORCHIDEE, TECO-SPRUCE, and VISIT become C sources under aCO_2 but remain near-neutral or C sinks under eCO_2 with transition thresholds varying among models (ORCHIDEE starting from +2.25°C, VISIT starting from +4.50°C, TECO-SPRUCE starting from +6.75°C, JULES starting from +9 °C). In contrast, DNDC and MWM remain C sinks or near-neutral at all warming levels.

Model responses of ecosystem components help to explain these NEE patterns. NPP increases with warming for some models (e.g., TECO-SPRUCE) and decreases for others (e.g., DNDC) from +0 °C to +9 °C. Across +2.25 to +9 °C, most models simulate HR increases that exceed gains in NPP, leading to more positive NEE (stronger C source) in many cases. Models differ in the extent to which eCO_2 mitigates these warming-induced losses, with stronger responses to eCO_2 in some models (e.g., ORCHIDEE, DNDC, VISIT) than others (e.g., CoupModel). CH_4 emissions generally increase with warming, although simulated magnitudes vary widely among models. CLM-Microbe consistently overestimates CH_4 fluxes across all warming levels relative to observations, whereas VISIT, LPX-Bern and ELM-SPRUCE consistently underestimate them.

https://doi.org/10.5194/egusphere-2026-5193
Preprint. Discussion started: 2 September 2026

464 The remaining models (DNDC, ELM-Microbe, LPJ-GUESS, PTEM, TECO-SPRUCE) transition
465 from overestimation at +0 °C to underestimation at +9 °C, with the transition occurring between
466 +4.5 and +6.75 °C.
467 Collectively, these results show that increasing temperature drives the peatland toward stronger C
468 losses, a pattern broadly captured by most models, while substantial inter-model differences
469 remain in the magnitude of responses and in how eCO_2 modulates the warming effect.

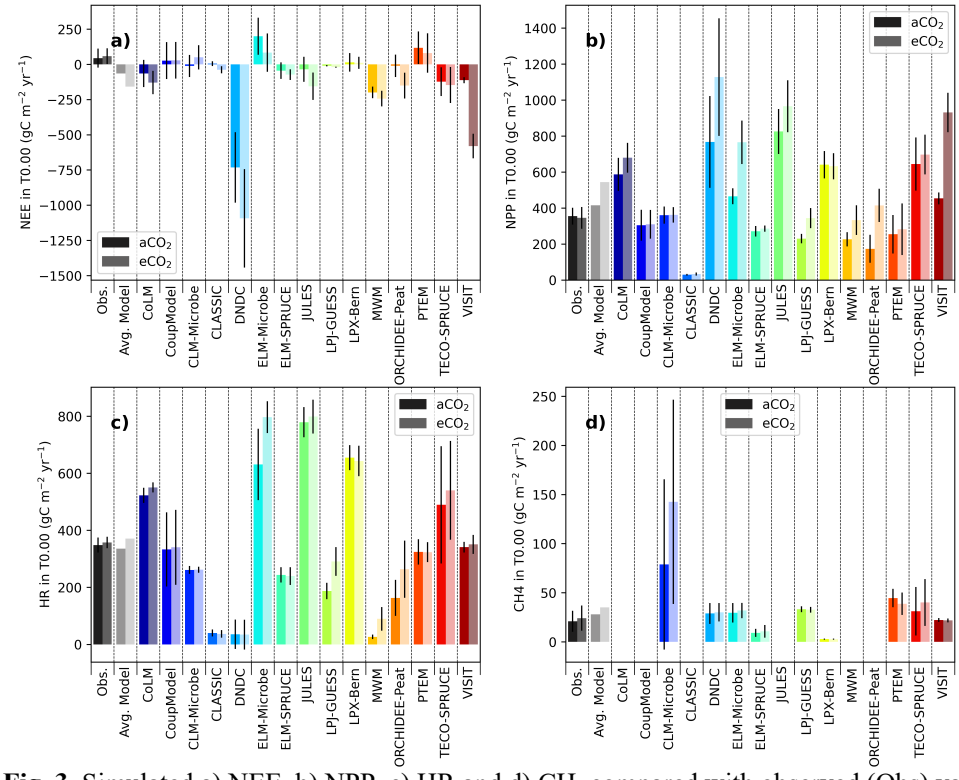

470
471 **Fig. 3.** Simulated a) NEE, b) NPP, c) HR and d) CH_4 compared with observed (Obs) values under
472 the +0 °C warming treatment at aCO_2 and eCO_2 conditions. Bars represent multi-year means
473 (2015-2021), and error bars denote interannual standard deviations of annual values. Note that
474 NEE includes the carbon equivalent of CH_4 emissions to account for their contribution to changes
475 in peat carbon stocks.
476
477 **3.2. Net ecosystem carbon exchange warming responses**
478
479 The slope-based temperature sensitivities of C fluxes summarize the responses shown in Fig. 3
480 and Supplemental Figs. S2-S5 and reveal substantial inter-model divergence in temperature-driven

https://doi.org/10.5194/egusphere-2026-5193
Preprint. Discussion started: 2 September 2026

C cycle feedbacks (Fig. 4). Most of the temperature sensitivities are statistically significant, except for CoLM (eCO_2 only), ELM_Microbe (aCO_2 only), JULES (eCO_2 only) and ORCHIDEE_Peat (both aCO_2 and eCO_2). Under aCO_2, the observed NEE increases significantly with temperature at a rate of 42±14 gC m^{-2} yr^{-1} $°C^{-1}$, while a significant but somewhat weaker response of 27±12 gC m^{-2} yr^{-1} $°C^{-1}$ is observed under eCO_2 (Fig. 4a). The multi-model mean, as well as CoLM (aCO_2 only), CLM-Microbe, ELM-Microbe (eCO_2 only), PTEM (aCO_2 only), and VISIT, exhibit warming responses within one standard deviation of the observed values, although ELM-Microbe and PTEM show more C loss under eCO_2 than aCO_2. DNDC and CoupModel display substantially larger positive sensitivities than observed (e.g., 108±38 and 62±21 gC m^{-2} yr^{-1} $°C^{-1}$ under aCO_2, respectively), with sensitivities further increasing under eCO_2. CoLM under eCO_2, as well as CLASSIC and LPJ-GUESS under both CO_2 treatments, exhibit positive sensitivities that underestimate observed levels. In contrast, ORCHIDEE and TECO-SPRUCE switch from positive under aCO_2 to negative under eCO_2 (TECO-SPRUCE reaching -21±10 gC m^{-2} yr^{-1} $°C^{-1}$ under eCO_2). LPJ-GUESS and MWM exhibit near-zero temperature sensitivities under both CO_2 conditions (generally below ~5 g C m^{-2} yr^{-1} $°C^{-1}$).

Observed NPP temperature sensitivities shift from slightly negative under aCO_2 (-7±8 gC m^{-2} yr^{-1} $°C^{-1}$) to positive under eCO_2 (10±7 gC m^{-2} yr^{-1} $°C^{-1}$) (Fig. 4b). ELM-SPRUCE and LPJ-GUESS are the two models exhibiting a similar sign change, though their positive responses under eCO_2 are small. LPX-Bern shifts from a near-zero temperature sensitivity under aCO_2 (< 1±20 gC m^{-2} yr^{-1} $°C^{-1}$) to a positive sensitivity under eCO_2 (~ 19±17 gC m^{-2} yr^{-1} $°C^{-1}$). MWM and TECO-SPRUCE remain consistently positive, CLASSIC, LPJ-GUESS, and PTEM are close to zero, whereas the multi-model average and most other models exhibit negative sensitivities under both CO_2 conditions. DNDC and ELM-Microbe show particularly strong negative responses, which become even more negative under eCO_2. NPP temperature sensitivities are statistically significant for all models except the observations under aCO_2, CoLM and ORCHIDEE_Peat under eCO_2, and PTEM under both CO_2 treatments.

The observed HR has positive temperature sensitivities under both CO_2 conditions, at +22 ± 7 g C m^{-2} yr^{-1} $°C^{-1}$ under aCO_2 and +22 ± 5 g C m^{-2} yr^{-1} $°C^{-1}$ under eCO_2 (Fig. 4c). CoupModel, CLASSIC, DNDC, ELM-SPRUCE, LPX-Bern, MWM, PTEM, TECO-SPRUCE, and VISIT also show positive HR temperature sensitivities, although their magnitudes vary widely (e.g., ~+52 g

https://doi.org/10.5194/egusphere-2026-5193
Preprint. Discussion started: 2 September 2026

C m^{-2} yr^{-1} $°C^{-1}$ in CoupModel versus ~+3 g C m^{-2} yr^{-1} $°C^{-1}$ in CLASSIC). In contrast, CoLM, CLM-Microbe, ELM-Microbe, JULES, and ORCHIDEE exhibit near-zero or negative HR temperature sensitivities. Observed HR temperature sensitivities are similar under aCO_2 and eCO_2, whereas modeled sensitivities show varying degrees of divergence between the two CO_2 conditions. LPJ-GUESS is the only model in which the HR temperature sensitivity changes sign, shifting from slightly negative under aCO_2 to positive under eCO_2. HR temperature sensitivities differ significantly from zero except for CoLM, JULES, and ORCHIDEE-Peat under both CO_2 conditions and LPJ-GUESS under eCO_2.

Observed CH_4 flux exhibits a consistently positive temperature sensitivity of 14 ± 8 g C m^{-2} yr^{-1} $°C^{-1}$ under both CO_2 conditions (Fig. 4d). PTEM and TECO-SPRUCE closely match these positive responses. In contrast, DNDC, ELM-Microbe, ELM-SPRUCE, LPJ-GUESS, LPX-Bern, and VISIT have much smaller CH_4 temperature sensitivities, whereas CLM-Microbe substantially overestimates the observed response, although its temperature sensitivity does not differ significantly from zero. CH_4 temperature sensitivities are similar between aCO_2 and eCO_2 in most models, whereas CLM-Microbe shows a lower temperature sensitivity under eCO_2 than under aCO_2.

Overall, most models (except ORCHIDEE, MWM and TECO-SPRUCE) capture the observed positive temperature sensitivities of NEE, although simulated magnitudes vary widely, ranging from strongly positive sensitivities in DNDC to weak responses in CLASSIC and LPJ-GUESS (Fig. 4a). These substantial variations cannot be explained solely by differences in the magnitude of baseline C fluxes, as larger discrepancies persist when temperature sensitivities are normalized by T0.00 mean NEE (Fig. S6a). NPP tends to decrease with warming in most models (except LPX-Bern, MWM, PTEM and TECO-SPRUCE), in contrast to the observed shift from negative to positive sensitivities between aCO_2 and eCO_2 (Fig. 4b), a pattern that is likewise reflected in normalized sensitivities (Fig. S6b). HR generally increases with temperature in both observations and nine of the fifteen models, whereas six models exhibit near-zero or negative sensitivities (Fig. 4c, Fig. S6c). Observed CH_4 fluxes exhibit strong positive temperature sensitivities under both CO_2 conditions, while modeled responses vary from strongly positive (CLM-Microbe, PTEM, TECO-SPRUCE) to nearly neutral (DNDC, ELM-Microbe, LPJ-GUESS, LPX-Bern, VISIT) (Fig. 4d, Fig. S6d). This wide range of temperature sensitivities, from strong C losses to minimal or

https://doi.org/10.5194/egusphere-2026-5193
Preprint. Discussion started: 2 September 2026

even negative responses, highlights the substantial uncertainty in projecting peatland C cycling under future warming and eCO_2.

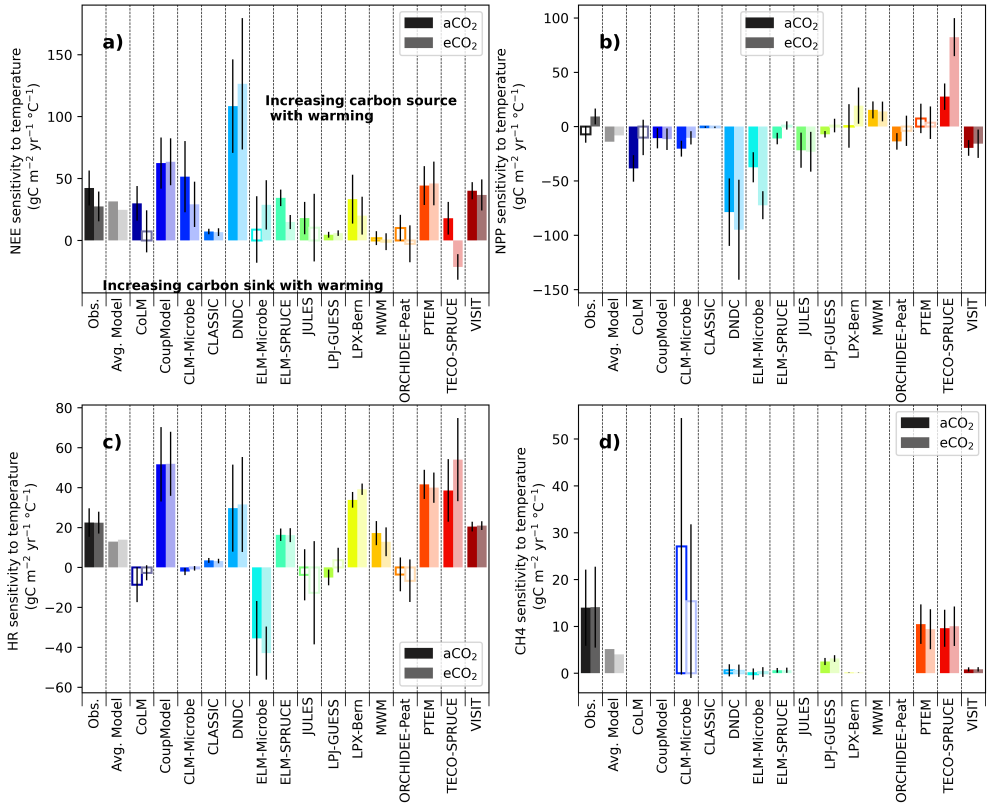

Fig. 4. Temperature sensitivities of a) NEE, b) NPP, c) HR, and d) CH_4 across the participating models compared with observed (Obs) values under both aCO_2 and eCO_2 conditions. Temperature sensitivities are least-squares linear regression slopes between annual mean air temperature and annual mean C fluxes, calculated separately for aCO_2 and eCO_2 conditions across all years and warming treatments. Error bars indicate ±1 standard deviation uncertainty of the estimated regression slopes (DeGroot & Schervish, 2018). Solid bars indicate slopes that differ significantly from zero ($p \leq 0.05$), whereas hollow bars indicate slopes that do not differ significantly from zero, based on Student's t-tests (DeGroot & Schervish, 2018).

3.3. Relationship between process representation and modeled responses

https://doi.org/10.5194/egusphere-2026-5193
Preprint. Discussion started: 2 September 2026

We evaluated how the representation of key ecosystem processes is associated with the magnitude and warming sensitivity of modeled C fluxes across the SPRUCE treatments using a Type-II ANOVA framework (Table 3). This approach tests the main effect of each factor while accounting for the influence of all others (Langsrud, 2003). Each analysis examined the relationship between the mean values or warming sensitivities of C fluxes and a set of Boolean indicators representing whether a given process is implemented in a model ("true") or not ("false"). Effect sizes are expressed as True minus False for process representations and elevated minus ambient for the CO_2 treatment; positive values indicate higher and negative values indicate lower modeled fluxes or warming sensitivities.

The analyzed processes include nutrient cycling (P; 5 of 15 models and N; 10 of 15 models), light competition (Light; 8 of 15 models), moss representation (Moss;12 of 15 models), dynamic peat representation (Peat; 5 of 15 models). CH_4 process representation was excluded as an explanatory factor because, in most models, enabling CH_4 simulation does not feed back on NEE, NPP, or HR. CH_4 flux was retained as a response variable. A Boolean indicator for elevated CO_2 was also included to control for differences between ambient and elevated CO_2 treatments.

PWT was implemented in the majority of participating models, leaving insufficient contrast between models with and without this feature. ACC and MT were implemented in only a small and overlapping subset of models, resulting in limited degrees of freedom and strong confounding with other structural features. Among the retained predictors, some process representations co-occur in the same models, but none has an identical presence/absence pattern across the model ensemble. Therefore, their effects are not perfectly confounded in the ANOVA. Even so, the results should be interpreted as statistical associations rather than definitive causal effects, because structural choices, parameterization, and model lineage are not fully independent. Statistically significant effects ($p \leq 0.05$) are indicated in bold in Table 3.

Across fluxes, nutrient cycling showed the most consistent associations with modeled C responses. Relative to models without N cycling, models with N cycling had significantly higher NPP by 323-369 g C m^{-2} yr^{-1} and higher HR by 340-533 g C m^{-2} yr^{-1} across all warming levels. At +9.00 °C, models with N cycling also had significantly higher NEE by 264 g C m^{-2} yr^{-1}, indicating stronger net C source behavior at the highest warming level. In contrast, models with

https://doi.org/10.5194/egusphere-2026-5193
Preprint. Discussion started: 2 September 2026

P cycling had significantly lower HR by 404-656 g C m^{-2} yr^{-1} across all warming levels, lower NEE by 317-365 g C m^{-2} yr^{-1} under +6.75 and +9.00 °C warming, and lower NPP by 317 g C m^{-2} yr^{-1} under +4.50 °C warming. These contrasting N and P associations suggest that different representations of nutrient limitation can strongly influence the balance between productivity and respiration.

Vegetation structural processes also contributed to model differences. Models with moss representation had significantly higher NEE under +4.50 to +9.00 °C warming by 274-442 g C m^{-2} yr^{-1} and higher HR over the same temperature range by 233-277 g C m^{-2} yr^{-1}. These patterns suggest that models including moss tend to simulate stronger C losses under warming, potentially through effects on litter inputs, productivity, and decomposition. Models with light competition had significantly lower NEE under the +0 °C treatment by 308 g C m^{-2} yr^{-1} and lower HR under the +0, +2.25, and +4.50 °C treatments by 169-283 g C m^{-2} yr^{-1}, indicating that vegetation competition is associated with differences in both net ecosystem exchange and respiratory fluxes.

Structural associations with warming sensitivity were more limited than those with mean fluxes. Dynamic peat representation was associated with a significantly lower NEE warming sensitivity by 36 g C m^{-2} yr^{-1} $°C^{-1}$, indicating weaker increases in net C loss with warming in models that include dynamic peat processes. For HR, models with light competition had a significantly higher warming sensitivity by 27 g C m^{-2} yr^{-1} $°C^{-1}$, whereas models with P cycling had a significantly lower warming sensitivity by 31 g C m^{-2} yr^{-1} $°C^{-1}$. No significant structural associations were detected for the warming sensitivity of NPP or CH_4 emissions.

For mean CH_4 emissions, significant associations with structural predictors occurred primarily at +2.25 and +4.50 °C warming. Models with N cycling had significantly higher CH_4 emissions by 44-64 g C m^{-2} yr^{-1} at these warming levels, whereas models with P cycling had significantly lower CH_4 emissions by 72 g C m^{-2} yr^{-1} at +4.50 °C. Models with dynamic peat representation had significantly lower CH_4 emissions by 65-87 g C m^{-2} yr^{-1} at +2.25 and +4.50 °C.

https://doi.org/10.5194/egusphere-2026-5193
Preprint. Discussion started: 2 September 2026

The elevated-CO_2 indicator, included in the ANOVA to account for differences between CO_2 treatments, was associated with significantly higher NPP only under +6.75 °C warming (+166 g C m^{-2} yr^{-1}), with no significant associations for NEE, HR, or CH_4 emissions.

Given differences in model parameterization, shared structural lineages, and the limited sample size, these ANOVA results cannot be attributed unambiguously to individual processes. Nevertheless, the analysis indicates that nutrient cycling, moss representation, light competition, and dynamic peat processes are associated with systematic differences in modeled peatland C fluxes and, in some cases, their warming sensitivities. These findings highlight the importance of consistent representation and calibration of key vegetation, nutrient, and peat processes for improving projections of peatland C dynamics under future environmental change.

Table 3. Estimated effect sizes of process representation (True − False) and CO_2 treatment (elevated − ambient) from the Type-II ANOVA. Bold values indicate statistically significant effects ($p \leq 0.05$). Process names are consistent with Fig. 2. The units are g C m^{-2} yr^{-1} for the mean values under each temperature treatment, and g C m^{-2} yr^{-1} $°C^{-1}$ for the warming response slope.

	Process	T0.00	T2.25	T4.50	T6.75	T9.00	slope
NEE	Light	**-308.23**	-235.33	-82.22	-144.14	-147.24	30.27
	Moss	250.62	272.33	**273.74**	**387.24**	**442.10**	15.42
	N	9.66	50.00	149.97	180.36	**263.81**	23.94
	P	-241.65	-271.78	-258.20	**-316.86**	**-365.08**	-4.10
	Peat	180.07	108.96	-41.34	-59.58	-76.66	**-36.45**
	CO_2	-93.13	-90.74	-92.13	-142.72	-120.77	-6.83
NPP	Light	-0.98	-23.82	-138.37	-55.10	-34.80	-9.52
	Moss	-58.96	-53.29	0.58	-80.37	-80.36	0.54
	N	**347.41**	**368.59**	**346.08**	**333.53**	**322.92**	4.54
	P	-161.83	-214.70	**-316.71**	-279.46	-295.38	-27.80
	Peat	-181.96	-177.37	-98.50	-75.74	-74.44	16.86
	CO_2	128.51	138.63	137.13	**166.35**	155.12	5.78
HR	Light	**-283.08**	**-225.62**	**-169.38**	-123.54	-95.27	**26.59**
	Moss	174.87	196.77	**232.89**	**242.77**	**277.24**	9.81
	N	**339.99**	**401.94**	**465.66**	**474.76**	**533.19**	24.94
	P	**-404.26**	**-490.29**	**-575.41**	**-601.58**	**-656.26**	**-31.32**
	Peat	2.98	-64.99	**-133.22**	-128.28	-144.67	-19.41
	CO_2	35.17	48.88	42.97	35.37	41.36	0.91
CH4	Light	-6.05	12.08	20.57	-28.71	-22.01	-2.93

https://doi.org/10.5194/egusphere-2026-5193
Preprint. Discussion started: 2 September 2026

	Moss	11.47	3.64	3.84	35.06	43.48	3.69
	N	13.86	**44.38**	**64.49**	83.30	94.43	9.84
	P	-0.32	-47.35	**-71.53**	-47.78	-63.96	-7.16
	Peat	-24.40	**-65.03**	**-87.32**	-75.94	-80.35	-6.97
	CO_2	7.10	3.39	1.26	-11.63	4.47	-1.13

4. Discussion

Northern peatlands have historically functioned as long-term net CO_2 sinks, playing a critical role in moderating the global Earth system (Frolking et al., 2011; Gallego-Sala et al., 2018; Helbig et al., 2022; Treat et al., 2019). However, our multi-model comparison reveals a wide range of responses in peatland C dynamics under experimental warming and eCO_2. This divergence reflects fundamental differences in how models represent and couple key processes, such as productivity, decomposition, methane cycling, and nutrient limitation, and how these processes interact under environmental perturbations (Hanson et al., 2020; Loisel et al., 2021; Zhao et al., 2022). In the following sections, we explore the implications of these contrasting responses for peatland vulnerability, uncertainties in C-climate feedbacks, and priorities for future model development.

4.1 Diverse simulated carbon dynamics in northern peatlands

To interpret the mechanisms underlying divergent model responses, we categorize the participating models into four functional types: (1) consistent carbon sources, (2) warming-induced sink-to-source transitions across both CO_2 treatments, (3) sink-to-source transitions under aCO_2 but sustained sinks under eCO_2, and (4) persistent C sinks or near-neutral systems. These groupings reflect underlying differences in structural assumptions, process representation, and sensitivities to temperature forcing.

CoupModel, ELM-Microbe, LPJ-Bern and PTEM consistently simulate peatlands as net C sources across all warming and CO_2 treatments, broadly aligning with SPRUCE observations. These models share detailed representations of peatland processes, including nutrient dynamics, moss physiology, and hydrological controls. Although the nutrient and CH_4 modules were deactivated for this intercomparison, CoupModel constrained hydrology using observed water table depths, thereby improving the realism of simulated HR (He et al., 2021;personal communication). ELM-

https://doi.org/10.5194/egusphere-2026-5193
Preprint. Discussion started: 2 September 2026

Microbe includes explicit microbial functional group-based CH_4 processes, accounting for dissolved organic carbon availability, multiple methanogenic and methanotrophic pathways, hydrogen production, and diverse CH_4 transport mechanisms (Ricciuto et al., 2021), in addition to N and P dynamics, moss physiology, and peatland hydrology (Shi et al., 2015 and 2021). LPX-Bern exhibits strong positive HR temperature sensitivity and negligible CH_4 emissions. Although NPP increases with warming, respiration dominates, resulting in persistent C source behavior across treatments. PTEM integrates peatland-specific plant functional types, peat elevation feedbacks, and aerobic and anaerobic decomposition pathways regulated by soil moisture (Zhao et al., 2022; Zhao and Zhuang, 2023, 2024). Collectively, these process representations promote respiratory C losses that outweigh warming-induced gains in productivity. Overall, these models illustrate how strong respiratory responses and detailed peatland process representation can produce persistent C-source behavior under warming.

A second group of models including CLASSIC, CLM-Microbe, CoLM, ELM-SPRUCE, and LPJ-GUESS exhibits warming-induced transitions from net C sinks to sources. In these models, warming alters the balance between NPP and HR in distinct ways. CLASSIC shows strong HR increases relative to NPP, but both fluxes are weaker than observed, resulting in a weak warming sensitivity in NEE (Fig. 4a-c). This behavior likely reflects the use here of empirical rather than dynamically coupled nutrient limitation, which may overestimate the nutrient constraint on HR and NPP responses to warming and CO_2 enrichment (Arora and Scinocca, 2016). CLM-Microbe maintains relatively stable HR under warming but experiences declining NPP and elevated CH_4 emissions, suggesting missing substrate or moisture feedbacks, or overly sensitive vegetation feedbacks. The contrasting responses of CLM-Microbe and ELM-Microbe, despite their shared CLM4.5 ancestry (Oleson et al., 2013), further suggest the strong influence of parameterization choices and nonlinear interactions arising from minor process changes. CoLM overestimates NPP at baseline, but warming-induced NPP reductions exceed HR declines, resulting in net C loss. ELM-SPRUCE incorporates coupled N and P cycling, with warming leading to NPP declines alongside HR and CH_4 emissions increases, and a prescribed reduction in moss cover, collectively driving a sink-to-source transition. LPJ-GUESS predicts concurrent declines in NPP and HR with warming, with stronger reductions in NPP and slight increases in CH_4 emissions, resulting in net

https://doi.org/10.5194/egusphere-2026-5193
Preprint. Discussion started: 2 September 2026

C loss. Together, these models demonstrate that sink-to-source transitions can emerge through multiple combinations of productivity decline, respiration enhancement, and methane responses.

A third set of models including JULES, ORCHIDEE, TECO-SPRUCE, and VISIT, transitions from C sinks to sources under aCO_2 but retains sink behavior under eCO_2, indicating strong CO_2 fertilization effects. ORCHIDEE shows NPP reductions under warming, likely reflecting Sphagnum sensitivity to temperature, but CO_2 fertilization partially buffers these losses under eCO_2. VISIT maintains high NPP across all warming scenarios under eCO_2, thereby preserving a net carbon sink. JULES, which lacks nutrient constraints, simulates stronger NPP under eCO_2 than aCO_2 and reduced NPP with warming, while failing to reproduce the observed positive HR response to warming. TECO-SPRUCE exhibits a nonlinear response, with warming weakening the sink under aCO_2 but enhancing C uptake under eCO_2, reflecting interactive effects among temperature, plant productivity, and microbial responses. These models emphasize the importance of CO_2 fertilization in moderating warming-induced C losses.

Finally, DNDC and MWM remain C sinks or near-neutral even under extreme warming. DNDC simulates steep NPP declines, and HR increases with warming under aCO_2. Under eCO_2, stable NPP sustains C uptake across most warming levels, with near-neutral behavior only under +9.00 °C. MWM incorporates peat cohort tracking and microbial decomposition processes, but represents only shrubs and mosses, lacking trees that constitute a substantial component of the SPRUCE ecosystem (Shao et al., 2022). This structural limitation may contribute to underestimated NPP under the lower warming treatments and persistent underestimation of HR (Fig. 3, Fig. S2-S5). In contrast, these models suggest that differences in vegetation representation, decomposition processes and parameterization can maintain sink behavior even under strong warming.

4.2 Benchmarking-related uncertainties in evaluating modeled peatland carbon dynamics

Our analysis highlights substantial uncertainties in benchmarking modeled peatland C dynamics against observations, arising from both observational constraints and asymmetries between observational and modeling frameworks. Field measurements of NEE, NPP, HR, and CH_4 fluxes used to benchmark the models are subject to substantial uncertainty because of spatial

https://doi.org/10.5194/egusphere-2026-5193
Preprint. Discussion started: 2 September 2026

heterogeneity, large interannual variability, heterogeneous vegetation composition, and methodological limitations (Bubier et al., 2003; Griffiths et al., 2017; Hanson et al., 2020; Moffat et al., 2007; Norby et al., 2019; Papale et al., 2006).

For instance, observed NEE under the lower warming treatments (+0 and +2.25 °C under aCO_2; Fig. 3 and Fig. S2) exhibited positive multi-year mean values. However, substantial interannual variability prevents a definitive classification of the peatland as a persistent C source under these conditions. More persistent C source behavior emerges under +2.25 °C with eCO_2 and under +4.5 °C or higher warming for both CO_2 treatments (Figs. S2-S5). These results reinforce previous studies showing that short-term interannual climate variability can obscure treatment effects in peatland C fluxes (Hanson et al., 2020). Several models (e.g., CoupModel, CLM-Microbe, CLASSIC, ELM-SPRUCE) similarly exhibit interannual NEE variability that exceeds their mean annual values at the lower warming levels (e.g., +0, +2.25 °C). Both observations and these models show a clearer transition toward persistent C-source behavior as warming increases.

Additional uncertainty arises from pretreatment differences among experimental chambers. Observed contrasts between aCO_2 and eCO_2 treatments may partly reflect background differences in vegetation composition and soil properties associated with small-scale spatial heterogeneity. Such pretreatment differences are not represented in the models, which branch from a common initial condition at the start of the experimental period (Sect. 2.2). While statistical adjustments can account for pretreatment effects in some variables (e.g., biomass and NPP; (Hanson et al., 2025)), this approach is more challenging for NEE and HR, where treatment signals are weaker, variability is larger, and underlying mechanisms are less directly observable.

A related limitation is that each warming × CO_2 treatment was applied to a single enclosure, preventing direct estimation of plot-to-plot variability under identical treatment conditions. Consequently, spatial heterogeneity among chambers cannot be separated from treatment effects. Pretreatment measurements indicate that differences in vegetation composition, peat properties, and ecosystem carbon fluxes existed among chambers before experimental manipulations began (Griffiths et al., 2017; Hanson et al., 2025). Although statistical adjustments can partially account for such differences for some variables, the absence of true treatment replication means that

https://doi.org/10.5194/egusphere-2026-5193
Preprint. Discussion started: 2 September 2026

uncertainty associated with small-scale spatial heterogeneity is difficult to quantify and remains an important consideration when evaluating model performance against observations.

Differences in response timescale further complicate model-data comparisons. In models, eCO_2 directly affects photosynthesis via stomatal and biochemical mechanisms, leading to immediate changes in NPP that can be readily detected in deterministic model simulations. In contrast, observed eCO_2 effects often emerge only after several years, as slow biomass accumulation, interacting environmental limitations, and measurement uncertainty can obscure early responses (Norby et al., 2024; Reich et al., 2018; Smith et al., 2014). On the other hand, the modeled HR responses to warming may emerge more slowly than those observed in the field, potentially contributing to the muted HR temperature sensitivity simulated by some models during the 2015-2021 period (Fig. 4c). One contributing factor may be that root exudate pools are not explicitly represented in most models, despite their rapid response to environmental change and their role as a highly labile C source for microbial respiration in the rhizosphere (Drake et al., 2011; Kuzyakov and Cheng, 2001).

A final source of discrepancy arises from differences in flux definitions between observed and modeled C fluxes. For example, observed NEE is derived from a combination of biomass increment estimates and chamber-based gas flux measurements, whereas models simulate continuous NEE based on internal ecosystem C balance equations. Similarly, observed NPP includes Sphagnum growth, and fine root production, but excludes shrub stem increment and some dormant-season production (Hanson et al., 2020). Consequently, observational estimates of NPP likely underestimate total ecosystem productivity and introduce additional uncertainty when compared with model-derived NPP. In addition, observed NPP also excludes root exudates, which may account for up to ~20% of NPP or NEE (Crow and Wieder, 2005; Wania et al., 2009). In contrast, most peatland models typically do not represent this C pathway explicitly and therefore may allocate a larger fraction of assimilated C to plant biomass than in the real world. These definitional mismatches complicate benchmarking efforts and highlight the need for consistent flux definitions and evaluation metrics in future model-experiment intercomparisons.

4.3 Model structural uncertainties

https://doi.org/10.5194/egusphere-2026-5193
Preprint. Discussion started: 2 September 2026

Our findings emphasize the critical role of structural uncertainty in shaping modeled C dynamics. The Type-II ANOVA indicates that the representations of nutrient cycling, vegetation structure (including moss representation and light competition), and dynamic peat processes systematically influence both the magnitude and, in some cases, the warming sensitivity of simulated C fluxes (Table 3). The influence of a given process on mean C fluxes does not necessarily correspond to its influence on warming sensitivities, highlighting the importance of interactions among vegetation, nutrients, and peat processes.

For example, light competition reduced mean HR and NEE under some warming treatments but increased the warming sensitivity of HR, whereas dynamic peat representation reduced the warming sensitivity of NEE (Table 3). The contrasting effects of N and P cycling on NEE and HR likely reflect differences in how nutrient limitation is represented across models, as well as differences in plant-microbe competition for soil nutrients (Arora and Scinocca, 2016). Moss representation also influenced simulated C fluxes by altering litter inputs, plant productivity, and substrate availability for decomposition. Although the underlying mechanisms differ among models, these results suggest that vegetation, nutrient, and peat process representations contribute to systematic differences in simulated peatland C dynamics. Given the limited number of participating models and the confounding factors between structural choices and parameterization, these inferred mechanisms should be interpreted cautiously. Nevertheless, the identified structural patterns provide a useful foundation for targeted model development and future model intercomparisons.

Differences in process representation and model parameterization appear to be more important than overall model complexity in explaining model behavior. For example, ELM-Microbe and PTEM reproduced the observed warming-induced transition toward stronger net carbon loss more closely than many other participating models, consistent with their detailed representations of peat soil processes, plant functional diversity (including mosses), and nutrient cycling (Ricciuto et al., 2021; Zhao and Zhuang, 2023). Several participating models within the CLM/ELM family, together with CoupModel, incorporated varying degrees of site-specific development, parameter calibration, or observational constraints informed by the SPRUCE experiment. These efforts illustrate the value of integrating long-term experimental observations into model development. However, because these models also differ substantially in model generation, process

https://doi.org/10.5194/egusphere-2026-5193
Preprint. Discussion started: 2 September 2026

795 representation, and parameterization, the relative contributions of site-specific development,
796 calibration, and structural differences cannot be isolated within the present intercomparison. In
797 contrast, CLASSIC exhibited relatively weak responses to warming and elevated CO_2, likely
798 reflecting its empirical downregulation of CO_2 fertilization and its nutrient limitation formulation
799 rather than overall model complexity. Despite incorporating relatively detailed process
800 representations, MWM and DNDC consistently simulated stronger C sinks than observed,
801 suggesting that differences in peatland-specific process representation, parameterization, or both
802 may contribute to these discrepancies (Shao et al., 2022, 2023). Overall, these contrasting
803 behaviors indicate that incorporating additional processes alone does not necessarily improve
804 model performance; rather, the representation, parameterization, and calibration of key vegetation,
805 nutrient, and peatland processes are the primary determinants of model skill.

806 Strong CO_2 fertilization responses further illustrate structural uncertainty. TECO-SPRUCE
807 exhibits a strong CO_2 fertilization effect that enhances NPP under elevated CO_2, although this
808 response may overestimate plant productivity if nutrient constraints are insufficiently represented.
809 In contrast, CoupModel and CLASSIC exhibit relatively weak NEE responses to elevated CO_2.
810 For CLASSIC, this behavior largely reflects its empirical downregulation of CO_2 fertilization and
811 nutrient limitation formulation, as mentioned earlier, whereas the comparatively weak CO_2
812 response in CoupModel likely reflects a simplified representation of CO_2 fertilization effects on
813 photosynthesis. Although these assumptions improve agreement with the SPRUCE observations,
814 they may reduce model generality across other peatland ecosystems. For the two microbe-enabled
815 models (ELM-Microbe and CLM-Microbe), the relatively weak sensitivity to elevated CO_2 may
816 arise from stronger microbial feedbacks that offset gains in plant productivity. Together, these
817 contrasting responses highlight the need for a unified benchmarking framework to systematically
818 evaluate how combinations of structural assumptions and parameter choices influence model
819 predictability.

820 Uncertainty in simulated CH_4 emissions remains particularly pronounced, reflecting differences in
821 hydrological representation, microbial parameterization, and the treatment of anaerobic processes
822 and water-table coupling across models (Estop-Aragonés et al., 2018; Melton et al., 2013).
823 Although CH_4 process representation was not identified as a primary driver of NEE, NPP, or HR
824 in the revised structural analysis, accurately simulating methane emissions remains essential for

https://doi.org/10.5194/egusphere-2026-5193
Preprint. Discussion started: 2 September 2026

evaluating peatland greenhouse-gas feedbacks. Continued coordination between long-term field measurements and standardized model evaluation will therefore be important for improving the representation of methane-related processes.

4.4 Influence of model parameter uncertainty

In addition to structural differences, inter-model divergence also reflects uncertainty in parameterization. Variations in parameters controlling HR sensitivity or the magnitude of CO_2 fertilization can substantially affect modeled C fluxes, even among structurally similar models (Lu and Ricciuto, 2019). The contrasting responses of CLM-Microbe and ELM-Microbe, despite their shared structural heritage, highlight the importance of parameter calibration using comprehensive observational datasets.

Because comprehensive parameter perturbation across all participating models is not feasible, we illustrate parameter-driven uncertainty using ELM-SPRUCE as an example. We perturb a suite of photosynthesis (flnr), C allocation (froot_leaf, stem_leaf), stomatal conductance (mbbopt), microbial decomposition (k_l3, decomp_depth_efolding, mino2lim, q10_mr, q10_hr), and CH_4 production (q10ch4, f_ch4) parameters within plausible ranges. Results for the +0 °C warming treatment under aCO_2 and eCO_2 conditions are shown in Figs. S7-8, with similar patterns observed across other warming levels.

NEE is most sensitive to allocation parameters of the spruce PFT (froot_leaf, stem_leaf), and to a lesser extent to moss photosynthetic capacity (flnr) and litter decomposition parameters (k_l3, q10_hr). CH_4 emissions are strongly influenced by the fraction of C allocated to CH_4 production (f_ch4), as well as by moss photosynthesis and allocation parameters. The parameter sensitivity analysis also indicates interactions among PFTs, with perturbations to spruce tree parameters influencing simulated NPP of tamarack, shrubs, and mosses (Figs. S7a, S8a). Consequently, models that do not represent the full suite of PFTs, such as MWM, which excludes trees, or TECO-SPRUCE, which represents a single PFT may not fully capture these interactions and their implications for C and nutrient cycling.

Overall, our results demonstrate that peatland models with diverse combinations of processes and parameters require careful validation, uncertainty quantification, and calibration to robustly project

https://doi.org/10.5194/egusphere-2026-5193
Preprint. Discussion started: 2 September 2026

responses to environmental change. Controlled experiments such as SPRUCE provide a unique opportunity to constrain temperature and CO_2 sensitivities beyond the range of historical variability. The parameter sensitivity analysis using ELM-SPRUCE illustrates how parameter choices can substantially influence simulated peatland C responses, complementing the structural uncertainty discussed in Section 4.3. More broadly, several participating models, particularly within the CLM/ELM family, together with CoupModel, incorporated varying degrees of site-specific process development, parameter calibration, or observational constraints informed by the SPRUCE experiment. These efforts illustrate the value of integrating long-term experimental observations into model development. However, because these models also differ substantially in model generation, process representation, and parameterization, the relative contributions of site-specific development, calibration, and structural differences cannot be isolated within the present intercomparison. Continued improvement in parameter calibration, together with better process representation, will reduce uncertainty and support more reliable projections of peatland C dynamics under future climate change.

4.5 Implications for climate feedbacks, ecosystem resilience, and future modeling

The SPRUCE-MIP results reaffirm that northern peatlands, despite their long-standing role as carbon sinks, are vulnerable to transitions under warming and eCO_2 (Koven et al., 2015a; Treat et al., 2019). Both observational and modeled evidence suggests that continued warming will likely shift these ecosystems toward net C loss, with the potential to introduce positive feedbacks to climate change through CO_2 and CH_4 emissions (Gallego-Sala et al., 2018; Koven et al., 2015b; Natali et al., 2019; Turetsky et al., 2020). However, the magnitude and even the direction of this feedback remain highly uncertain, as evidenced by the wide range of simulated NEE temperature sensitivities across the model ensemble.

This uncertainty arises from fundamental differences in how key peatland processes are represented and coupled in current models. Results from the process-based analysis highlight the importance of vegetation structure (light competition and moss representation), nutrient cycling (N and P), and peat processes in shaping mean C fluxes and, in some cases, their responses to warming. These processes regulate the balance between productivity and HR and modulate how C losses are partitioned between CO_2 and CH_4 pathways. Disagreement among models is

https://doi.org/10.5194/egusphere-2026-5193
Preprint. Discussion started: 2 September 2026

particularly pronounced for CH_4 emissions and CO_2 fertilization responses. More than a decade after the WETCHIMP and WETCHIMP-WSL intercomparison projects identified substantial divergence in modeled wetland CH_4 (Bohn et al., 2015; Melton et al., 2013), the present SPRUCE-MIP results indicate that comparable levels of disagreement persist, now extending beyond CH_4 to include net carbon balance and warming sensitivity. Structural differences among models continue to produce widely divergent projections. This persistence suggests that improving peatland projections requires not only additional process complexity, but more systematic evaluation of how key processes are coupled and parameterized across models. Although most models simulate enhanced NPP under eCO_2, many appear to overestimate this effect relative to observations at SPRUCE under low-warming conditions, suggesting incomplete representation of interacting constraints such as nutrient availability and vegetation-microbe competition.

Recent observational studies further suggest that peatland vulnerability may be amplified when warming and increased CO_2 emissions interact with hydrological extremes. For example, (Quan et al., 2025) using observations from the SPRUCE experiment, (Quan et al., 2025) using observations from the SPRUCE experiment, demonstrated that drought-induced C losses in peatlands are exacerbated under combined warming and elevated CO_2, highlighting the importance of compound climate stressors that extend beyond warming or CO_2 enrichment alone. Together with the SPRUCE warming experiment, such findings indicate that future peatland C responses and associated climate feedbacks are likely governed by interacting controls on productivity, decomposition, CH_4 cycling, and ecosystem water status, rather than by single drivers in isolation.

From an ecosystem resilience perspective, the model ensemble reveals markedly different capacities for resistance and persistence under warming. Some models transition to net C sources under relatively modest temperature increases, whereas others remain sinks even under +9 °C warming. This divergence raises critical questions about the credibility and transferability of resilience projections derived from either individual models or multi-model ensembles. Although the multi-model mean generally captures the observed transition toward stronger C loss with warming, it masks substantial differences among individual models in both the magnitude and mechanisms of the response. Consequently, agreement between the ensemble mean and observations should not necessarily be interpreted as evidence that the underlying process representations are correct. Importantly, it suggests that resilience metrics based solely on mean

https://doi.org/10.5194/egusphere-2026-5193
Preprint. Discussion started: 2 September 2026

carbon balance may be insufficient, and that transient responses, compensating flux changes, and recovery trajectories must also be considered. Another challenge lies in addressing the decadal-to-millennial process timescales associated with peat C dynamics and distinguishing short-term responses examined here from long-term peat accumulation and loss. Peat C pools accumulate and turn over on centennial to millennial timescales, whereas experimental manipulations such as SPRUCE necessarily operate over years to decades. This disparity complicates model spin-up, initialization, and evaluation, particularly when short-term flux responses are used to infer longer-term peatland C-climate feedbacks (Müller and Joos, 2021). The spread in modeled responses identified here therefore reflects not only differences in process representation, but also how individual models translate short-term perturbations into longer-term C balance trajectories. In this context, SPRUCE-MIP is not intended to benchmark long-term peat accumulation directly, but rather to diagnose structural sensitivities and emergent behaviors that shape near-term responses and condition longer-term outcomes.

These findings point to several priorities for future model development and evaluation. First, improved representation of vegetation structure and functional diversity, including interactions among mosses, shrubs, and trees, is essential for capturing interactions between productivity, litter inputs, and decomposition. Trait-based or multi-PFT frameworks provide promising pathways for resolving these interactions. Second, nutrient cycling and CH_4 processes require more consistent and mechanistic treatment to reduce biases in CO_2 fertilization responses and CH_4 emissions. Third, manipulative experiments such as SPRUCE should be more fully leveraged for model calibration and benchmarking. Beyond warming and CO_2 treatments, water table depth manipulation at SPRUCE was initiated recently, providing a new opportunity to directly constrain hydrological controls on peatland carbon cycling. Although these data are not analyzed in the present study, they have strong potential to improve model representations of aerobic versus anaerobic decomposition and methane production.

Future benchmarking efforts should move beyond mean annual fluxes to include interannual variability, component flux sensitivities, and indicators of resistance and recovery. Combining controlled manipulations with naturally occurring extremes, such as drought events, offers a powerful framework for evaluating model performance under conditions that more closely resemble future climate variability. Finally, peatland model evaluation should extend beyond

https://doi.org/10.5194/egusphere-2026-5193
Preprint. Discussion started: 2 September 2026

comparisons with contemporary flux measurements to also consider the current global distribution of peat C (e.g., (Xu et al., 2018)) and reconstructions of peatland area and C stock evolution over the deglacial period and the Holocene (e.g., (Loisel et al., 2017; Yu et al., 2010)). Such long-term constraints provide an important test of whether models reproduce both present-day peat C stocks and the processes governing their accumulation over millennial timescales. Together, these advances will be critical for reducing uncertainty in projections of peatland C responses and their associated climate feedbacks and for improving the reliability of Earth system models in representing the vulnerability of this globally significant carbon reservoir.

5. Conclusions

This SPRUCE-MIP intercomparison reveals substantial divergence in simulated northern peatland C responses to warming and elevated CO_2, underscoring persistent uncertainty in model-based projections of peatland behavior under environmental change. Across the model ensemble, responses range from persistent C sinks to consistent C sources, with multiple forms of sink-to-source transitions emerging under increasing temperature and CO_2 enrichment. These contrasting outcomes highlight the sensitivity of peatland C balance to differences in process representation, parameterization, and environmental forcing.

Based on their behavior across warming and CO_2 treatments, models can be broadly grouped into four functional response types: (i) models that simulate peatlands as net C sources across all conditions; (ii) models that transition from sinks to sources under warming regardless of CO_2 level; (iii) models that transition to sources only under aCO_2 but remain sinks under eCO_2, reflecting strong CO_2 fertilization effects; and (iv) models that maintain persistent sinks or near-neutral C balance even under extreme warming. The coexistence of these response types within a single intercomparison emphasizes that peatland vulnerability cannot be inferred from temperature or CO_2 forcing alone.

The spread in simulated responses is driven by differences in the representation and coupling of key ecosystem processes. Vegetation structure, including light competition and moss representation, nutrient cycling, and dynamic peat processes exert systematic influences on mean C fluxes and, in some cases, their warming sensitivities. Models differ markedly in how warming

https://doi.org/10.5194/egusphere-2026-5193
Preprint. Discussion started: 2 September 2026

alters the balance between productivity and HR and in how C losses are partitioned among ecosystem pathways. Although eCO_2 generally enhances modeled productivity, many models simulate stronger fertilization effects than supported by observations at SPRUCE under low-warming conditions, pointing to incomplete representation of interacting nutrient, vegetation, and microbial constraints. Parameter sensitivity analyses conducted for ELM-SPRUCE further indicate that parameter choices can substantially modulate the magnitude of simulated C flux responses.

Together, these findings indicate that future peatland C responses to warming and elevated CO_2 will be governed by interacting biological, biogeochemical, and physical processes, and may be strongly modulated under compound climatic stressors. Reducing uncertainty will require coordinated advances in long-term manipulative experiments, model development, and complementary constraints from reconstructions of past peatland extent and C accumulation. Experiments such as SPRUCE provide critical constraints on process sensitivities beyond the historical climate envelope, while emerging observations, including drought impacts and newly initiated water table manipulation, offer valuable opportunities to evaluate ecosystem resistance, recovery, and nonlinear responses. Improving the representation of vegetation functional diversity, nutrient-microbe interactions, hydrological and peatland processes, CH_4 related processes, and transient ecosystem responses will be essential for strengthening confidence in projections of peatland C dynamics. Ultimately, SPRUCE-MIP demonstrates that translating short-term experimental responses into longer-term projections of peatland C-climate feedbacks depends critically on how models represent and couple vegetation dynamics, nutrient cycling, hydrology, and peat processes. Although CH_4 process representation was not identified as a primary structural driver of ecosystem C balance, uncertainties in simulated CH_4 emissions remain an important source of divergence in projected greenhouse-gas feedbacks.

Data availability

The observational and model datasets used in this study are available from the corresponding author upon reasonable request.

Author contributions

XS, DMR, and JM designed the study and SPRUCE-MIP protocol. XS and YW performed the multi-model analyses, and YW contributed to the initial development and drafting of the process-

https://doi.org/10.5194/egusphere-2026-5193
Preprint. Discussion started: 2 September 2026

representation analysis in Sect. 3.3. XS prepared the initial manuscript draft. XS, JRM, FJ, QS, YL, JZhou, XX, JZhang, DH, QZ, YY, CQ, HH, MW, SS, XL, YD, AI, NC, AH, RHT, and EJB conducted model simulations, provided model results, and contributed model descriptions. YH contributed to Figs. 1 and 2 and assisted with references. PJH, NAG, VS, and MAM provided observational datasets. PET contributed to the interpretation and analysis of model results. JRM and FJ provided substantial comments that improved the manuscript. All authors reviewed and edited the manuscript.

Competing interests

The authors declare that they have no conflict of interest.

Acknowledgements

This study was conducted as a part of the Oak Ridge National Laboratory (ORNL) Terrestrial Ecosystem Sciences Scientific Focus Area which is funded by the U.S. Department of Energy (DOE) Office of Biological and Environmental Research, Environmental Systems Science program. ORNL is managed by UT-Battelle, LLC, for the U.S. DOE under contract DE-AC05-1008 00OR22725. The simulations with ELM-SPRUCE model and all multi-model data analyses were conducted using the cades-baseline supercomputer, which is part of the Oak Ridge Leadership Computing Facility. The simulations for other models were done by the external modeling team representative co-authors, supported by their own resources, and using open-source data.

F.J. and Q.S. were supported by the Swiss National Science Foundation (grant 200020 200511). LPX-Bern simulations were performed on UBELIX (https://www.id.unibe.ch/hpc), the HPC cluster at the University of Bern.
C.Q. acknowledges support from the CALIPSO (Carbon Loss in Plant Soils and Oceans) project, funded through the generosity of Eric and Wendy Schmidt by recommendation of the Schmidt Futures program.

D. H. was supported by the DOE RDPP grant DE-SC0023335.

N.C. acknowledges funding from the Swedish Research Council FORMAS grant (contract nos. 2019-01151 and 2023-00310). LPJ-GUESS simulations were enabled by resources provided by the Swedish National Infrastructure for Computing (SNIC) at the Lund University Centre for Scientific and Technical Computing (Lunarc), project nos. LU 2026/2-43, LU 2026/12-5 and by resources at Linköping University, project nos. NAISS 2026/3-223, 2025/22-1776, NAISS 2025/23-732. N.C. also acknowledges support from the strategic research areas Modeling the Regional and Global Earth System (MERGE) and Biodiversity and Ecosystem Services in a Changing Climate (BECC) at Lund University.

E.J.B and R.H.T were supported by the Met Office Hadley Centre Climate Programme (HCCP) funded by the UK Department for Business, Innovation, Science and Trade (DBIST).
R.H.T was also supported by UK Research & Innovation's Natural Environment Research Council (UKRI-NERC) Mothership peatland project (Improving MOdelling approaches to assess

https://doi.org/10.5194/egusphere-2026-5193
Preprint. Discussion started: 2 September 2026

climate change-related THresholds and Ecological Range SHIfts in the Earth's Peatland ecosystems), through grant NE/V018418/1.

ChatGPT (OpenAI) was used to assist with language editing and improve the readability of the manuscript.

6. References

Arora, V. K. and Scinocca, J. F.: Constraining the strength of the terrestrial CO_2 fertilization effect in the Canadian Earth system model version 4.2 (CanESM4.2), Geosci. Model Dev., 9, 2357–2376, https://doi.org/10.5194/gmd-9-2357-2016, 2016.

Bohn, T. J., Melton, J. R., Ito, A., Kleinen, T., Spahni, R., Stocker, B. D., Zhang, B., Zhu, X., Schroeder, R., and Glagolev, M. V: WETCHIMP-WSL: intercomparison of wetland methane emissions models over West Siberia, Biogeosciences, 12, 3321–3349, 2015.

Bubier, J. L., Bhatia, G., Moore, T. R., Roulet, N. T., and Lafleur, P. M.: Spatial and temporal variability in growing-season net ecosystem carbon dioxide exchange at a large peatland in Ontario, Canada, Ecosystems, 353–367, 2003.

Burke, E. J., Chadburn, S. E., and Ekici, A.: A vertical representation of soil carbon in the JULES land surface scheme (vn4. 3_permafrost) with a focus on permafrost regions, Geosci. Model Dev., 10, 959–975, 2017.

Chaudhary, N., Miller, P. A., and Smith, B.: Modelling past, present and future peatland carbon accumulation across the pan-Arctic region, Biogeosciences, 14, 4023–4044, 2017.

Chaudhary, N., Westermann, S., Lamba, S., Shurpali, N., Sannel, A. B. K., Schurgers, G., Miller, P. A., and Smith, B.: Modelling past and future peatland carbon dynamics across the pan-Arctic, Glob. Chang. Biol., 26, 4119–4133, 2020.

Chaudhary, N., Tuovinen, J., Kou, D., Deb Burman, P. K., Lodh, A., Lamba, S., Shurpali, N., Schurgers, G., Page, S. E., and Westermann, S.: Peatlands have the potential to emerge as significant contributors to future climate warming, J. Geophys. Res. Biogeosci., 131, e2025JG009540, 2026.

Crichton, K. A., Anderson, K., Fewster, R. E., Charman, D. J., Garneau, M., Väliranta, M., Mleczko, M., Handley, J. N., Hodson, S., and Parker, R. E.: Satellite data indicates recent Arctic peatland expansion with warming, Commun. Earth Environ., 6, 461, 2025.

Crow, S. E. and Wieder, R. K.: Sources of CO2 emission from a northern peatland: root respiration, exudation, and decomposition, Ecology, 86, 1825–1834, 2005.

Dai, Y., Wei, N., Yuan, H., Zhang, S., Shangguan, W., Liu, S., Lu, X., and Xin, Y.: Evaluation of Soil Thermal Conductivity Schemes for Use in Land Surface Modeling, J. Adv. Model. Earth Syst., 11, 3454–3473, https://doi.org/https://doi.org/10.1029/2019MS001723, 2019.

Dargie, G. C., Lewis, S. L., Lawson, I. T., Mitchard, E. T. A., Page, S. E., Bocko, Y. E., and Ifo, S. A.: Age, extent and carbon storage of the central Congo Basin peatland complex, Nature, 542, 86–90, 2017.

DeGroot, M. H. and Schervish, M. J.: Probability and Statistics, 4th ed., Pearson, New York, 2018.

Drake, J. E., Gallet-Budynek, A., Hofmockel, K. S., Bernhardt, E. S., Billings, S. A., Jackson, R. B., Johnsen, K. S., Lichter, J., McCarthy, H. R., and McCormack, M. L.: Increases in the

https://doi.org/10.5194/egusphere-2026-5193
Preprint. Discussion started: 2 September 2026

flux of carbon belowground stimulate nitrogen uptake and sustain the long-term enhancement of forest productivity under elevated CO2, Ecol. Lett., 14, 349–357, 2011.

Duque, A., Peña, M. A., Cuesta, F., González-Caro, S., Kennedy, P., Phillips, O. L., Calderón-Loor, M., Blundo, C., Carilla, J., and Cayola, L.: Mature Andean forests as globally important carbon sinks and future carbon refuges, Nat. Commun., 12, 2138, 2021.

Estop-Aragonés, C., Cooper, M. D. A., Fisher, J. P., Thierry, A., Garnett, M. H., Charman, D. J., Murton, J. B., Phoenix, G. K., Treharne, R., Sanderson, N. K., Burn, C. R., Kokelj, S. V, Wolfe, S. A., Lewkowicz, A. G., Williams, M., and Hartley, I. P.: Limited release of previously-frozen C and increased new peat formation after thaw in permafrost peatlands, Soil Biol. Biochem., 118, 115–129, https://doi.org/https://doi.org/10.1016/j.soilbio.2017.12.010, 2018.

Frolking, S., Roulet, N. T., Tuittila, E., Bubier, J. L., Quillet, A., Talbot, J., and Richard, P. J. H.: A new model of Holocene peatland net primary production, decomposition, water balance, and peat accumulation, Earth System Dynamics, 1, 1–21, 2010.

Frolking, S., Talbot, J., Jones, M. C., Treat, C. C., Kauffman, J. B., Tuittila, E.-S., and Roulet, N.: Peatlands in the Earth's 21st century climate system, Environmental Reviews, 19, 371–396, https://doi.org/10.1139/a11-014, 2011.

Frolking, S., Talbot, J., and Subin, Z. M.: Exploring the relationship between peatland net carbon balance and apparent carbon accumulation rate at century to millennial time scales, Holocene, 24, 1167–1173, 2014.

Gallego-Sala, A. V, Charman, D. J., Brewer, S., Page, S. E., Prentice, I. C., Friedlingstein, P., Moreton, S., Amesbury, M. J., Beilman, D. W., and Björck, S.: Latitudinal limits to the predicted increase of the peatland carbon sink with warming, Nat. Clim. Chang., 8, 907–913, 2018.

Griffiths, N. A., Hanson, P. J., Ricciuto, D. M., Iversen, C. M., Jensen, A. M., Malhotra, A., McFarlane, K. J., Norby, R. J., Sargsyan, K., Sebestyen, S. D., Shi, X., Walker, A. P., Ward, E. J., Warren, J. M., and Weston, D. J.: Temporal and Spatial Variation in Peatland Carbon Cycling and Implications for Interpreting Responses of an Ecosystem-Scale Warming Experiment, Soil Science Society of America Journal, 81, 1668–1688, https://doi.org/https://doi.org/10.2136/sssaj2016.12.0422, 2017.

Hanson, P. J., Gill, A. L., Xu, X., Phillips, J. R., Weston, D. J., Kolka, R. K., Riggs, J. S., and Hook, L. A.: Intermediate-scale community-level flux of CO2 and CH4 in a Minnesota peatland: putting the SPRUCE project in a global context, Biogeochemistry, 129, 255–272, https://doi.org/10.1007/s10533-016-0230-8, 2016.

Hanson, P. J., Riggs, J. S., Nettles, W. R., Phillips, J. R., Krassovski, M. B., Hook, L. A., Gu, L., Richardson, A. D., Aubrecht, D. M., and Ricciuto, D. M.: Attaining whole-ecosystem warming using air and deep-soil heating methods with an elevated CO 2 atmosphere, Biogeosciences, 14, 861–883, 2017.

Hanson, P. J., Griffiths, N. A., Iversen, C. M., Norby, R. J., Sebestyen, S. D., Phillips, J. R., Chanton, J. P., Kolka, R. K., Malhotra, A., and Oleheiser, K. C.: Rapid net carbon loss from a whole-ecosystem warmed peatland, Agu Advances, 1, e2020AV000163, 2020.

Hanson, P. J., Griffiths, N. A., Salmon, V. G., Birkebak, J. M., Warren, J. M., Phillips, J. R., Guilliams, M. P., Oleheiser, K. C., Jones, M. W., Jones, N. J., Enterkine, J., Glenn, N. F., and Pearson, K. J.: Peatland Plant Community Changes in Annual Production and Composition Through 8 Years of Warming Manipulations Under Ambient and Elevated

https://doi.org/10.5194/egusphere-2026-5193
Preprint. Discussion started: 2 September 2026

CO2 Atmospheres, J. Geophys. Res. Biogeosci., 130, e2024JG008511, https://doi.org/https://doi.org/10.1029/2024JG008511, 2025.

He, H., Jansson, P.-E., and Gärdenäs, A. I.: CoupModel (v6.0): an ecosystem model for coupled phosphorus, nitrogen, and carbon dynamics – evaluated against empirical data from a climatic and fertility gradient in Sweden, Geosci. Model Dev., 14, 735–761, https://doi.org/10.5194/gmd-14-735-2021, 2021.

Hedwall, P., Brunet, J., and Rydin, H.: Peatland plant communities under global change: negative feedback loops counteract shifts in species composition, Ecology, 98, 150–161, 2017.

Helbig, M., Waddington, J. M., Alekseychik, P., Amiro, B. D., Aurela, M., Barr, A. G., Black, T. A., Blanken, P. D., Carey, S. K., Chen, J., Chi, J., Desai, A. R., Dunn, A., Euskirchen, E. S., Flanagan, L. B., Forbrich, I., Friborg, T., Grelle, A., Harder, S., Heliasz, M., Humphreys, E. R., Ikawa, H., Isabelle, P.-E., Iwata, H., Jassal, R., Korkiakoski, M., Kurbatova, J., Kutzbach, L., Lindroth, A., Löfvenius, M. O., Lohila, A., Mammarella, I., Marsh, P., Maximov, T., Melton, J. R., Moore, P. A., Nadeau, D. F., Nicholls, E. M., Nilsson, M. B., Ohta, T., Peichl, M., Petrone, R. M., Petrov, R., Prokushkin, A., Quinton, W. L., Reed, D. E., Roulet, N. T., Runkle, B. R. K., Sonnentag, O., Strachan, I. B., Taillardat, P., Tuittila, E.-S., Tuovinen, J.-P., Turner, J., Ueyama, M., Varlagin, A., Wilmking, M., Wofsy, S. C., and Zyrianov, V.: Increasing contribution of peatlands to boreal evapotranspiration in a warming climate, Nat. Clim. Chang., 10, 555–560, https://doi.org/10.1038/s41558-020-0763-7, 2020.

Helbig, M., Živković, T., Alekseychik, P., Aurela, M., El-Madany, T. S., Euskirchen, E. S., Flanagan, L. B., Griffis, T. J., Hanson, P. J., and Hattakka, J.: Warming response of peatland CO2 sink is sensitive to seasonality in warming trends, Nat. Clim. Chang., 12, 743–749, 2022.

Huang, Y., Jiang, J., Ma, S., Ricciuto, D., Hanson, P. J., and Luo, Y.: Soil thermal dynamics, snow cover, and frozen depth under five temperature treatments in an ombrotrophic bog: Constrained forecast with data assimilation, J. Geophys. Res. Biogeosci., 122, 2046–2063, 2017.

Huang, Y., Nicholson, D., Huang, B., and Cassar, N.: Global estimates of marine gross primary production based on machine learning upscaling of field observations, Global Biogeochem. Cycles, 35, e2020GB006718, 2021.

(IPCC), I. P. on C. C.: Climate Change 2022 – Impacts, Adaptation and Vulnerability: Working Group II Contribution to the Sixth Assessment Report of the Intergovernmental Panel on Climate Change, Cambridge University Press, Cambridge, https://doi.org/DOI: 10.1017/9781009325844, 2023.

Ito, A. and Inatomi, M.: Use of a process-based model for assessing the methane budgets of global terrestrial ecosystems and evaluation of uncertainty, Biogeosciences, 9, 759–773, 2012.

Jansson, P.-E. and Moon, D. S.: A coupled model of water, heat and mass transfer using object orientation to improve flexibility and functionality, Environmental Modelling & Software, 16, 37–46, 2001.

Koven, C. D., Schuur, E. A. G., Schädel, C., Bohn, T. J., Burke, E. J., Chen, G., Chen, X., Ciais, P., Grosse, G., Harden, J. W., Hayes, D. J., Hugelius, G., Jafarov, E. E., Krinner, G., Kuhry, P., Lawrence, D. M., MacDougall, A. H., Marchenko, S. S., McGuire, A. D., Natali, S. M., Nicolsky, D. J., Olefeldt, D., Peng, S., Romanovsky, V. E., Schaefer, K. M., Strauss, J.,

https://doi.org/10.5194/egusphere-2026-5193
Preprint. Discussion started: 2 September 2026

Treat, C. C., and Turetsky, M.: A simplified, data-constrained approach to estimate the permafrost carbon–climate feedback, Philosophical Transactions of the Royal Society A: Mathematical, Physical and Engineering Sciences, 373, 20140423, https://doi.org/10.1098/rsta.2014.0423, 2015a.

Koven, C. D., Lawrence, D. M., and Riley, W. J.: Permafrost carbon− climate feedback is sensitive to deep soil carbon decomposability but not deep soil nitrogen dynamics, Proceedings of the National Academy of Sciences, 112, 3752–3757, 2015b.

Kuzyakov, Y. and Cheng, W.: Photosynthesis controls of rhizosphere respiration and organic matter decomposition, Soil Biol. Biochem., 33, 1915–1925, 2001.

Kwon, M. J., Ballantyne, A., Ciais, P., Qiu, C., Salmon, E., Raoult, N., Guenet, B., Göckede, M., Euskirchen, E. S., and Nykänen, H.: Lowering water table reduces carbon sink strength and carbon stocks in northern peatlands, Glob. Chang. Biol., 28, 6752–6770, 2022.

Leifeld, J. and Menichetti, L.: The underappreciated potential of peatlands in global climate change mitigation strategies, Nat. Commun., 9, 1071, https://doi.org/10.1038/s41467-018-03406-6, 2018.

Li, C., Frolking, S., and Frolking, T. A.: A model of nitrous oxide evolution from soil driven by rainfall events: 1. Model structure and sensitivity, Journal of Geophysical Research: Atmospheres, 97, 9759–9776, 1992.

Loisel, J., van Bellen, S., Pelletier, L., Talbot, J., Hugelius, G., Karran, D., Yu, Z., Nichols, J., and Holmquist, J.: Insights and issues with estimating northern peatland carbon stocks and fluxes since the Last Glacial Maximum, Earth. Sci. Rev., 165, 59–80, 2017.

Loisel, J., Gallego-Sala, A. V, Amesbury, M. J., Magnan, G., Anshari, G., Beilman, D. W., Benavides, J. C., Blewett, J., Camill, P., and Charman, D. J.: Expert assessment of future vulnerability of the global peatland carbon sink, Nat. Clim. Chang., 11, 70–77, 2021.

Lu, D. and Ricciuto, D.: Efficient surrogate modeling methods for large-scale Earth system models based on machine-learning techniques, Geosci. Model Dev., 12, 1791–1807, 2019.

Mathison, C., Burke, E., Hartley, A. J., Kelley, D. I., Burton, C., Robertson, E., Gedney, N., Williams, K., Wiltshire, A., and Ellis, R. J.: Description and evaluation of the JULES-ES set-up for ISIMIP2b, Geosci. Model Dev., 16, 4249–4264, 2023.

McDonald, R. M., Moore, P. A., Helbig, M., and Waddington, J. M.: Reduced Net CO2 Uptake During Dry Summers in a Boreal Shield Peatland, J. Geophys. Res. Biogeosci., 128, e2022JG006923, https://doi.org/https://doi.org/10.1029/2022JG006923, 2023.

Melton, J. R., Wania, R., Hodson, E. L., Poulter, B., Ringeval, B., Spahni, R., Bohn, T., Avis, C. A., Beerling, D. J., and Chen, G.: Present state of global wetland extent and wetland methane modelling: conclusions from a model inter-comparison project (WETCHIMP), Biogeosciences, 10, 753–788, 2013.

Melton, J. R., Arora, V. K., Wisernig-Cojoc, E., Seiler, C., Fortier, M., Chan, E., and Teckentrup, L.: CLASSIC v1.0: the open-source community successor to the Canadian Land Surface Scheme (CLASS) and the Canadian Terrestrial Ecosystem Model (CTEM) – Part 1: Model framework and site-level performance, Geosci. Model Dev., 13, 2825–2850, https://doi.org/10.5194/gmd-13-2825-2020, 2020.

Moffat, A. M., Papale, D., Reichstein, M., Hollinger, D. Y., Richardson, A. D., Barr, A. G., Beckstein, C., Braswell, B. H., Churkina, G., and Desai, A. R.: Comprehensive comparison of gap-filling techniques for eddy covariance net carbon fluxes, Agric. For. Meteorol., 147, 209–232, 2007.

https://doi.org/10.5194/egusphere-2026-5193
Preprint. Discussion started: 2 September 2026

Müller, J. and Joos, F.: Committed and projected future changes in global peatlands–continued transient model simulations since the Last Glacial Maximum, Biogeosciences, 18, 3657–3687, 2021.

Natali, S. M., Watts, J. D., Rogers, B. M., Potter, S., Ludwig, S. M., Selbmann, A.-K., Sullivan, P. F., Abbott, B. W., Arndt, K. A., and Birch, L.: Large loss of CO2 in winter observed across the northern permafrost region, Nat. Clim. Chang., 9, 852–857, 2019.

Norby, R. J., De Kauwe, M. G., Domingues, T. F., Duursma, R. A., Ellsworth, D. S., Goll, D. S., Lapola, D. M., Luus, K. A., MacKenzie, A. R., Medlyn, B. E., Pavlick, R., Rammig, A., Smith, B., Thomas, R., Thonicke, K., Walker, A. P., Yang, X., and Zaehle, S.: Model–data synthesis for the next generation of forest free-air CO2 enrichment (FACE) experiments, New Phytologist, 209, 17–28, https://doi.org/https://doi.org/10.1111/nph.13593, 2016.

Norby, R. J., Childs, J., Hanson, P. J., and Warren, J. M.: Rapid loss of an ecosystem engineer: Sphagnum decline in an experimentally warmed bog, Ecol. Evol., 9, 12571–12585, https://doi.org/https://doi.org/10.1002/ece3.5722, 2019.

Norby, R. J., Loader, N. J., Mayoral, C., Ullah, S., Curioni, G., Smith, A. R., Reay, M. K., van Wijngaarden, K., Amjad, M. S., Brettle, D., Crockatt, M. E., Denny, G., Grzesik, R. T., Hamilton, R. L., Hart, K. M., Hartley, I. P., Jones, A. G., Kourmouli, A., Larsen, J. R., Shi, Z., Thomas, R. M., and MacKenzie, A. R.: Enhanced woody biomass production in a mature temperate forest under elevated CO2, Nat. Clim. Chang., 14, 983–988, https://doi.org/10.1038/s41558-024-02090-3, 2024.

O'Donnell, J. A., Jorgenson, M. T., Harden, J. W., McGuire, A. D., Kanevskiy, M. Z., and Wickland, K. P.: The effects of permafrost thaw on soil hydrologic, thermal, and carbon dynamics in an Alaskan peatland, Ecosystems, 15, 213–229, 2012.

Ofiti, N. O. E., Schmidt, M. W. I., Abiven, S., Hanson, P. J., Iversen, C. M., Wilson, R. M., Kostka, J. E., Wiesenberg, G. L. B., and Malhotra, A.: Climate warming and elevated CO2 alter peatland soil carbon sources and stability, Nat. Commun., 14, 7533, 2023.

Oleson, K. W., Lawrence, D. M., Bonan, G. B., Fisher, R. A., Lawrence, P. J., and Muszala, S. P.: Technical description of version 4.5 of the Community Land Model (CLM), Technical description of version 4.5 of the Community Land Model (CLM)(2013) NCAR/TN-503+ STR, 503, 2013.

Papale, D., Reichstein, M., Aubinet, M., Canfora, E., Bernhofer, C., Kutsch, W., Longdoz, B., Rambal, S., Valentini, R., and Vesala, T.: Towards a standardized processing of Net Ecosystem Exchange measured with eddy covariance technique: algorithms and uncertainty estimation, Biogeosciences, 3, 571–583, 2006.

Qiu, C., Zhu, D., Ciais, P., Guenet, B., Krinner, G., Peng, S., Aurela, M., Bernhofer, C., Brümmer, C., and Bret-Harte, S.: ORCHIDEE-PEAT (revision 4596), a model for northern peatland CO 2, water and energy fluxes on daily to annual scales, Geoscientific Model Development Discussions, 2017, 1–56, 2017.

Qiu, C., Zhu, D., Ciais, P., Guenet, B., Peng, S., Krinner, G., Tootchi, A., Ducharne, A., and Hastie, A.: Modelling northern peatland area and carbon dynamics since the Holocene with the ORCHIDEE-PEAT land surface model (SVN r5488), Geosci. Model Dev., 12, 2961–2982, 2019.

Qiu, C., Zhu, D., Ciais, P., Guenet, B., and Peng, S.: The role of northern peatlands in the global carbon cycle for the 21st century, Global Ecology and Biogeography, 29, 956–973, 2020.

https://doi.org/10.5194/egusphere-2026-5193
Preprint. Discussion started: 2 September 2026

Quan, Q., Zhou, J., Hanson, P. J., Ricciuto, D., Sebestyen, S. D., Weston, D. J., Chanton, J. P., Wilson, R. M., Kostka, J. E., and Zhou, Y.: Drought-induced peatland carbon loss exacerbated by elevated CO2 and warming, Science (1979)., 390, 367–370, 2025.

Reich, P. B., Hobbie, S. E., Lee, T. D., and Pastore, M. A.: Unexpected reversal of C3 versus C4 grass response to elevated CO2 during a 20-year field experiment, Science (1979)., 360, 317–320, 2018.

Ribeiro, K., Pacheco, F. S., Ferreira, J. W., de Sousa-Neto, E. R., Hastie, A., Krieger Filho, G. C., Alvalá, P. C., Forti, M. C., and Ometto, J. P.: Tropical peatlands and their contribution to the global carbon cycle and climate change, Glob. Chang. Biol., 27, 489–505, 2021.

Ricciuto, D. M., Xu, X., Shi, X., Wang, Y., Song, X., Schadt, C. W., Griffiths, N. A., Mao, J., Warren, J. M., and Thornton, P. E.: An integrative model for soil biogeochemistry and methane processes: I. Model structure and sensitivity analysis, J. Geophys. Res. Biogeosci., 126, e2019JG005468, 2021.

Richardson, A. D., Hufkens, K., Milliman, T., Aubrecht, D. M., Furze, M. E., Seyednasrollah, B., Krassovski, M. B., Latimer, J. M., Nettles, W. R., Heiderman, R. R., Warren, J. M., and Hanson, P. J.: Ecosystem warming extends vegetation activity but heightens vulnerability to cold temperatures, Nature, 560, 368–371, https://doi.org/10.1038/s41586-018-0399-1, 2018.

Riley, W. J., Subin, Z. M., Lawrence, D. M., Swenson, S. C., Torn, M. S., Meng, L., Mahowald, N. M., and Hess, P.: Barriers to predicting changes in global terrestrial methane fluxes: analyses using CLM4Me, a methane biogeochemistry model integrated in CESM, Biogeosciences, 8, 1925–1953, 2011.

Sebestyen, S. D., Dorrance, C., Olson, D. M., Verry, E. S., Kolka, R. K., Elling, A. E., and Kyllander, R.: Long-term monitoring sites and trends at the Marcell Experimental Forest, Peatland biogeochemistry and watershed hydrology at the Marcell Experimental Forest, 1, 15–71, 2011.

Shao, S., Wu, J., He, H., and Roulet, N.: Integrating McGill Wetland Model (MWM) with peat cohort tracking and microbial controls, Science of the Total Environment, 806, 151223, 2022.

Shao, S., Wu, J., He, H., Moore, T. R., Bubier, J., Larmola, T., Juutinen, S., and Roulet, N. T.: Ericoid mycorrhizal fungi mediate the response of ombrotrophic peatlands to fertilization: a modeling study, New Phytologist, 238, 80–95, 2023.

Shi, X., Ricciuto, D. M., Thornton, P. E., Xu, X., Yuan, F., Norby, R. J., Walker, A. P., Warren, J. M., Mao, J., and Hanson, P. J.: Extending a land-surface model with Sphagnum moss to simulate responses of a northern temperate bog to whole ecosystem warming and elevated CO 2, Biogeosciences, 18, 467–486, 2021.

Skye, J., Melton, J. R., Goldblatt, C., Gallego-Sala, A., Garneau, M., and Winton, S.: PeatDepth-ML: a global map of peat depth predicted using machine learning, Biogeosciences, 23, 2959–2983, 2026.

Smith, S. D., Charlet, T. N., Zitzer, S. F., Abella, S. R., Vanier, C. H., and Huxman, T. E.: Long-term response of a Mojave Desert winter annual plant community to a whole-ecosystem atmospheric CO2 manipulation (FACE), Glob. Chang. Biol., 20, 879–892, 2014.

Spahni, R., Joos, F., Stocker, B. D., Steinacher, M., and Yu, Z. C.: Transient simulations of the carbon and nitrogen dynamics in northern peatlands: From the Last Glacial Maximum to the 21st century, Climate of the Past, 9, 1287–1308, 2013.

https://doi.org/10.5194/egusphere-2026-5193
Preprint. Discussion started: 2 September 2026

St-Hilaire, F., Wu, J., Roulet, N. T., Frolking, S., Lafleur, P. M., Humphreys, E. R., and Arora, V.: McGill wetland model: evaluation of a peatland carbon simulator developed for global assessments, Biogeosciences, 7, 3517–3530, 2010.

Treat, C. C., Wollheim, W. M., Varner, R. K., Grandy, A. S., Talbot, J., and Frolking, S.: Temperature and peat type control CO2 and CH4 production in Alaskan permafrost peats, Glob. Chang. Biol., 20, 2674–2686, https://doi.org/https://doi.org/10.1111/gcb.12572, 2014.

Treat, C. C., Kleinen, T., Broothaerts, N., Dalton, A. S., Dommain, R., Douglas, T. A., Drexler, J. Z., Finkelstein, S. A., Grosse, G., Hope, G., Hutchings, J., Jones, M. C., Kuhry, P., Lacourse, T., Lähteenoja, O., Loisel, J., Notebaert, B., Payne, R. J., Peteet, D. M., Sannel, A. B. K., Stelling, J. M., Strauss, J., Swindles, G. T., Talbot, J., Tarnocai, C., Verstraeten, G., Williams, C. J., Xia, Z., Yu, Z., Väliranta, M., Hättestrand, M., Alexanderson, H., and Brovkin, V.: Widespread global peatland establishment and persistence over the last 130,000 y, Proceedings of the National Academy of Sciences, 116, 4822–4827, https://doi.org/10.1073/pnas.1813305116, 2019.

Treat, C. C., Jones, M. C., Alder, J., Sannel, A. B. K., Camill, P., and Frolking, S.: Predicted vulnerability of carbon in permafrost peatlands with future climate change and permafrost thaw in Western Canada, J. Geophys. Res. Biogeosci., 126, e2020JG005872, 2021.

Turetsky, M. R., Donahue, Wf., and Benscoter, B. W.: Experimental drying intensifies burning and carbon losses in a northern peatland, Nat. Commun., 2, 514, 2011.

Turetsky, M. R., Abbott, B. W., Jones, M. C., Anthony, K. W., Olefeldt, D., Schuur, E. A. G., Grosse, G., Kuhry, P., Hugelius, G., and Koven, C.: Carbon release through abrupt permafrost thaw, Nat. Geosci., 13, 138–143, 2020.

Wang, S., Ma, J., Rydin, H., Mallik, A., Yu, Z., Wang, M., Sun, Z., and Bu, Z.: Climate Controls Cold-But Not Warm-Adapted Sphagnum Distribution and Carbon Sink Capacity, Glob. Chang. Biol., 32, e71006, 2026.

Wania, R., Ross, I., and Prentice, I. C.: Integrating peatlands and permafrost into a dynamic global vegetation model: 2. Evaluation and sensitivity of vegetation and carbon cycle processes, Global Biogeochem. Cycles, 23, 2009.

Weng, E. and Luo, Y.: Soil hydrological properties regulate grassland ecosystem responses to multifactor global change: A modeling analysis, J. Geophys. Res. Biogeosci., 113, https://doi.org/https://doi.org/10.1029/2007JG000539, 2008.

Xie, A., Zhu, J., Kang, S., Qin, X., Xu, B., and Wang, Y.: Polar amplification comparison among Earth's three poles under different socioeconomic scenarios from CMIP6 surface air temperature, Sci. Rep., 12, 16548, https://doi.org/10.1038/s41598-022-21060-3, 2022.

Xu, J., Morris, P. J., Liu, J., and Holden, J.: PEATMAP: Refining estimates of global peatland distribution based on a meta-analysis, Catena (Amst)., 160, 134–140, 2018.

Xu, X., Elias, D. A., Graham, D. E., Phelps, T. J., Carroll, S. L., Wullschleger, S. D., and Thornton, P. E.: A microbial functional group-based module for simulating methane production and consumption: Application to an incubated permafrost soil, J. Geophys. Res. Biogeosci., 120, 1315–1333, https://doi.org/https://doi.org/10.1002/2015JG002935, 2015.

Yu, Z., Loisel, J., Brosseau, D. P., Beilman, D. W., and Hunt, S. J.: Global peatland dynamics since the Last Glacial Maximum, Geophys. Res. Lett., 37, 2010.

Yu, Z. C.: Northern peatland carbon stocks and dynamics: a review, Biogeosciences, 9, 4071–4085, https://doi.org/10.5194/bg-9-4071-2012, 2012.

https://doi.org/10.5194/egusphere-2026-5193
Preprint. Discussion started: 2 September 2026

1359 Zhao, B. and Zhuang, Q.: Peatlands and their carbon dynamics in northern high latitudes from
1360 1990 to 2300: a process-based biogeochemistry model analysis, Biogeosciences, 20, 251–
1361 270, 2023.
1362 Zhao, B. and Zhuang, Q.: Nitrogen Cycling Feedback on Carbon Dynamics Leads to Greater
1363 CH4 Emissions and Weaker Cooling Effect of Northern Peatlands, Global Biogeochem.
1364 Cycles, 38, e2023GB007978, https://doi.org/https://doi.org/10.1029/2023GB007978, 2024.
1365 Zhao, B., Zhuang, Q., and Frolking, S.: Modeling Carbon Accumulation and Permafrost
1366 Dynamics of Northern Peatlands Since the Holocene, J. Geophys. Res. Biogeosci., 127,
1367 e2022JG007009, https://doi.org/https://doi.org/10.1029/2022JG007009, 2022.
1368